



US011326174B2

(12) **United States Patent**
Myers et al.

(10) **Patent No.:** **US 11,326,174 B2**
(45) **Date of Patent:** **May 10, 2022**

(54) **ENGINEERED YEAST STRAINS ENABLING ANAEROBIC XYLOSE FERMENTATION DECOUPLED FROM MICROBIAL GROWTH**

FOREIGN PATENT DOCUMENTS

WO WO 2017158189 A1 * 9/2017 C07K 14/395

(71) Applicant: **Wisconsin Alumni Research Foundation**, Madison, WI (US)

OTHER PUBLICATIONS

(72) Inventors: **Kevin S Myers**, Madison, WI (US); **Audrey P Gasch**, Madison, WI (US)

Brown et al., How nutritional status signalling coordinates metabolism and lignocellulolytic enzyme secretion. *Fungal Genetics Biol.*, 2014, vol. 72: 48-63. (Year: 2014).*

(73) Assignee: **Wisconsin Alumni Research Foundation**, Madison, WI (US)

Caspeta et al., Modifying Yeast Tolerance to inhibitory Conditions of ethanol Production Processes. *Frontiers Bioeng. Biotechnol.*, 2015, vol. 3, Article 184, pp. 1-15 (Year: 2015).*

(*) Notice: Subject to any disclaimer, the term of this patent is extended or adjusted under 35 U.S.C. 154(b) by 220 days.

Hu et al., The localization and concentration of thePDE2-encoded high-affinity cAMP phosphodiesterase is regulated by cAMP-dependent protein kinase A in the yeast *Saccharomyces cerevisiae*. *FEMS Yeast Res.*, 2010, vol. 10: 177-187. (Year: 2010).*

(21) Appl. No.: **16/542,758**

Morawska et al., An expanded tool kit for the auxin-inducible degron system in budding yeast. *Yeast*, 2013, vol. 30: 341-351. (Year: 2013).*

(22) Filed: **Aug. 16, 2019**

Myers et al., Rewired cellular signaling coordinates sugar and hypoxic responses for anaerobic xylose fermentation in yeast. *PLoS Genetics*, Mar. 11, 2019, pp. 1-33. (Year: 2019).*

(65) **Prior Publication Data**

US 2020/0056194 A1 Feb. 20, 2020

Peck et al., Yeast bcy1 mutants with stationary phase-specific defects. *Curr Genet.*, 1997, vol. 32: 8392. (Year: 1997).*

Related U.S. Application Data

(60) Provisional application No. 62/719,346, filed on Aug. 17, 2018.

* cited by examiner

(51) **Int. Cl.**
C12N 15/81 (2006.01)
C12N 15/90 (2006.01)
C12P 7/10 (2006.01)

Primary Examiner — Ganapathirama Raghu

(74) *Attorney, Agent, or Firm* — Schwegman Lundberg & Woessner, P.A.

(52) **U.S. Cl.**
CPC **C12N 15/81** (2013.01); **C12N 15/905** (2013.01); **C12P 7/10** (2013.01)

(57) **ABSTRACT**

The present invention relates to materials and methods for the production of ethanol. More particularly, the present invention provides genetically modified strains of *Saccharomyces cerevisiae* exhibiting decreased level of BCY1 protein activity and capable of anaerobic fermentation of xylose into ethanol without the need for cell growth. Also provided are methods of using such genetically engineered yeast strains for improved anaerobic xylose fermentation in the yeast for industrial-scale production of various fuels, chemical feedstocks, and synthetic polymers.

(58) **Field of Classification Search**
CPC C12P 7/10; C12N 15/905; C12N 15/81; C07K 14/395
See application file for complete search history.

(56) **References Cited**

U.S. PATENT DOCUMENTS

2019/0106469 A1 * 4/2019 Gasch C12P 7/10

9 Claims, 15 Drawing Sheets
(15 of 15 Drawing Sheet(s) Filed in Color)

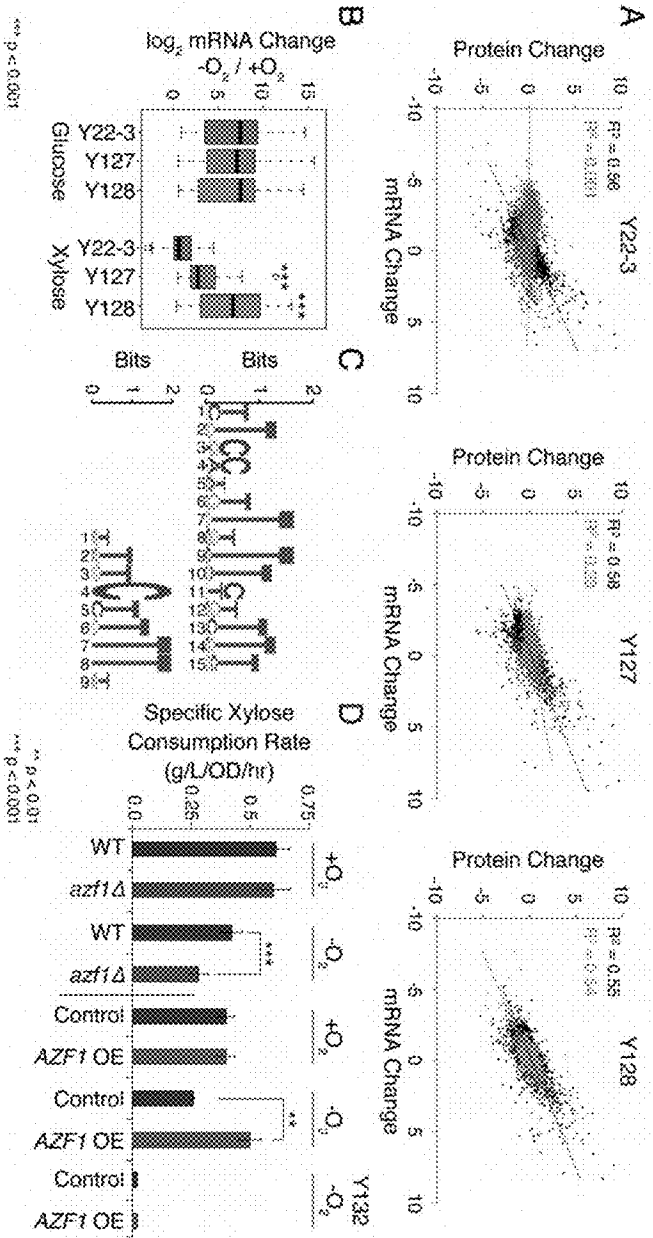


FIG. 1

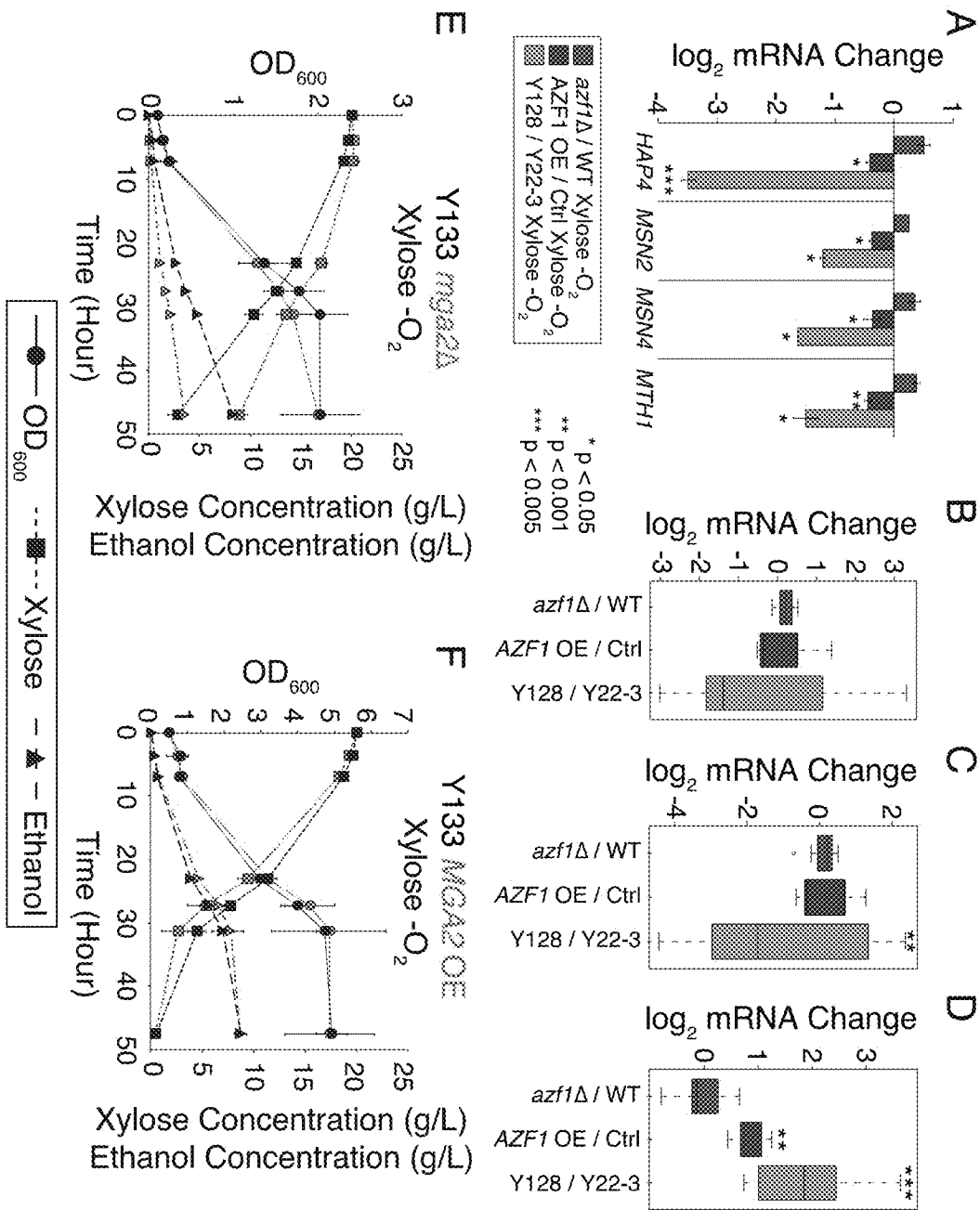


FIG. 2

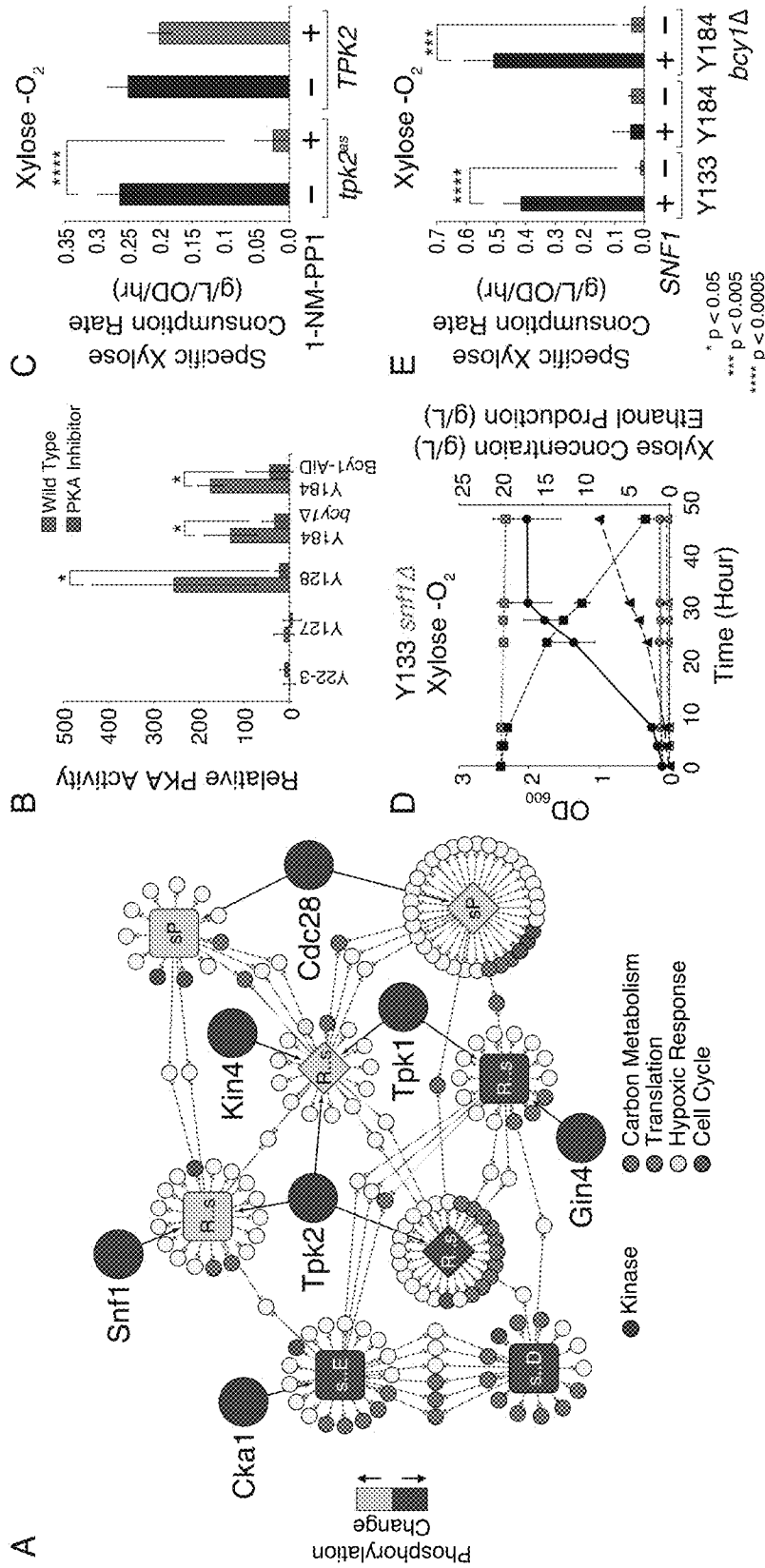


FIG. 3

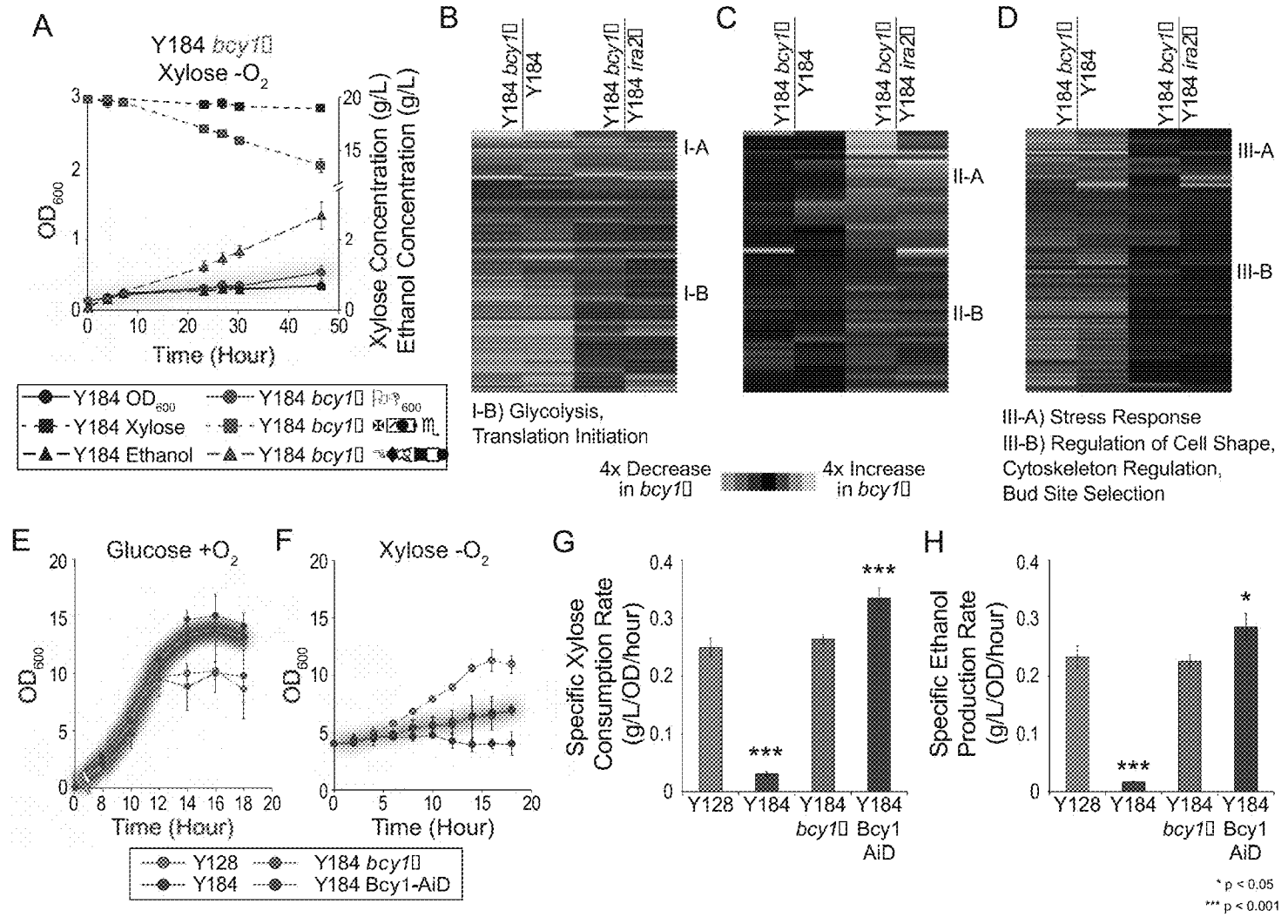


FIG. 4

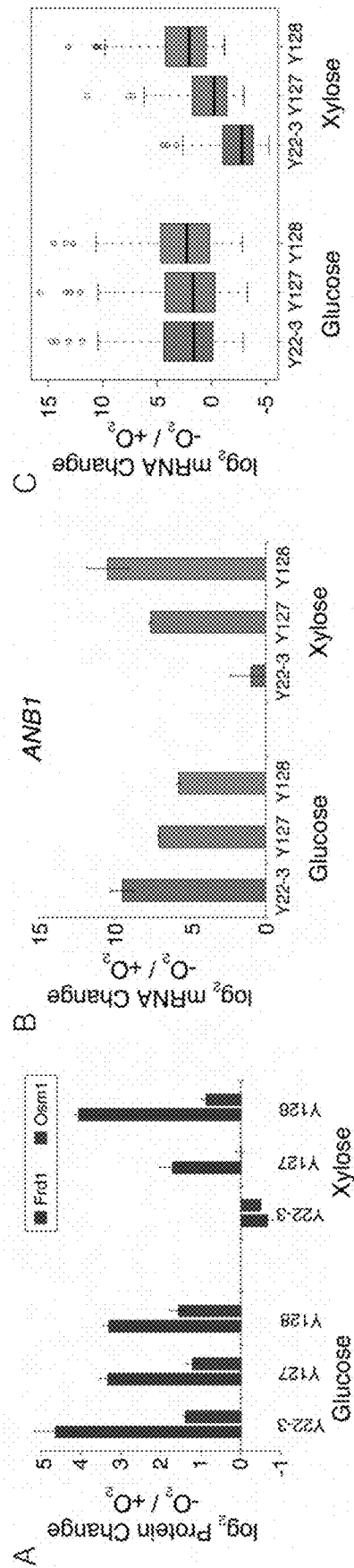


FIG. 6

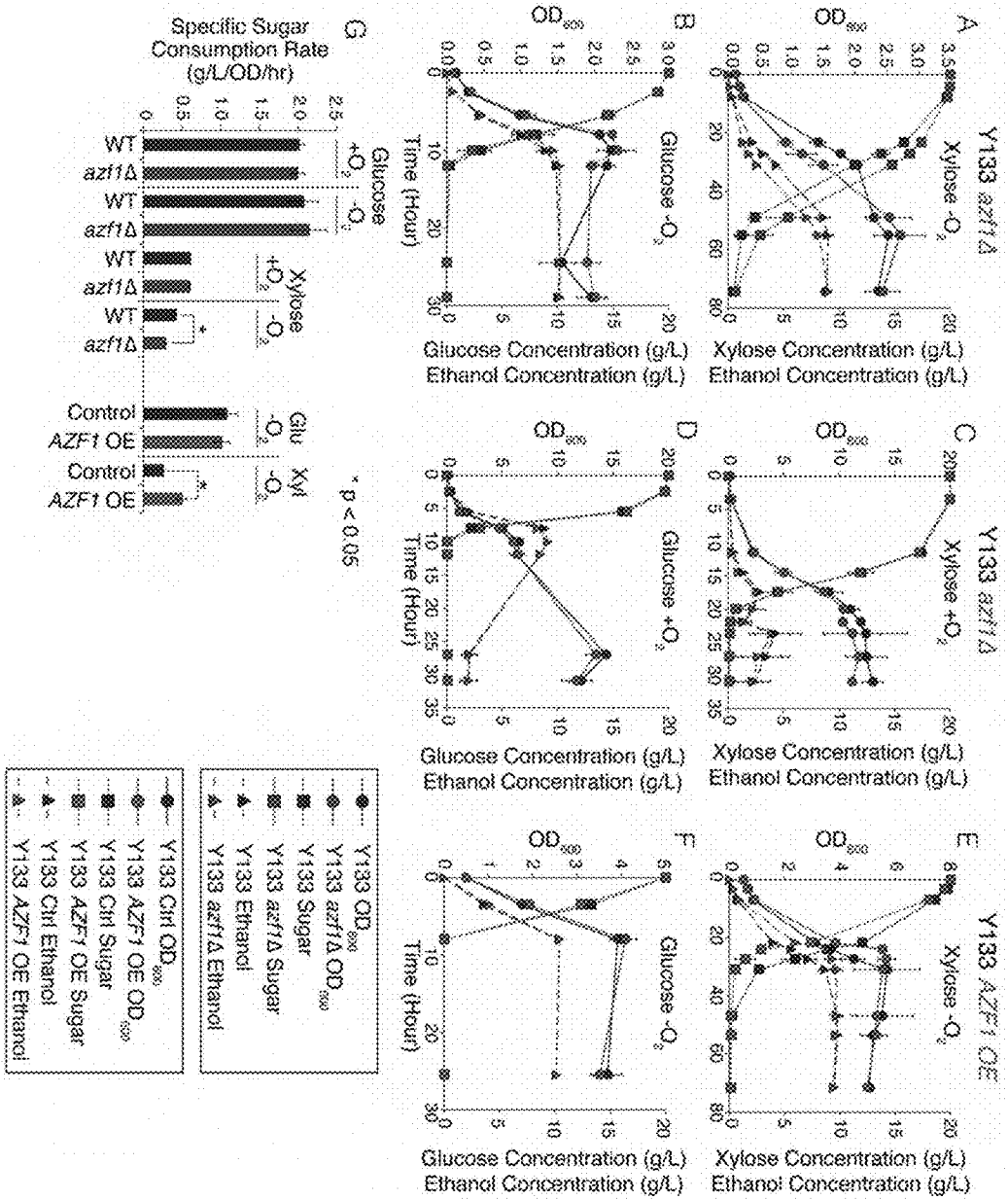


FIG. 7

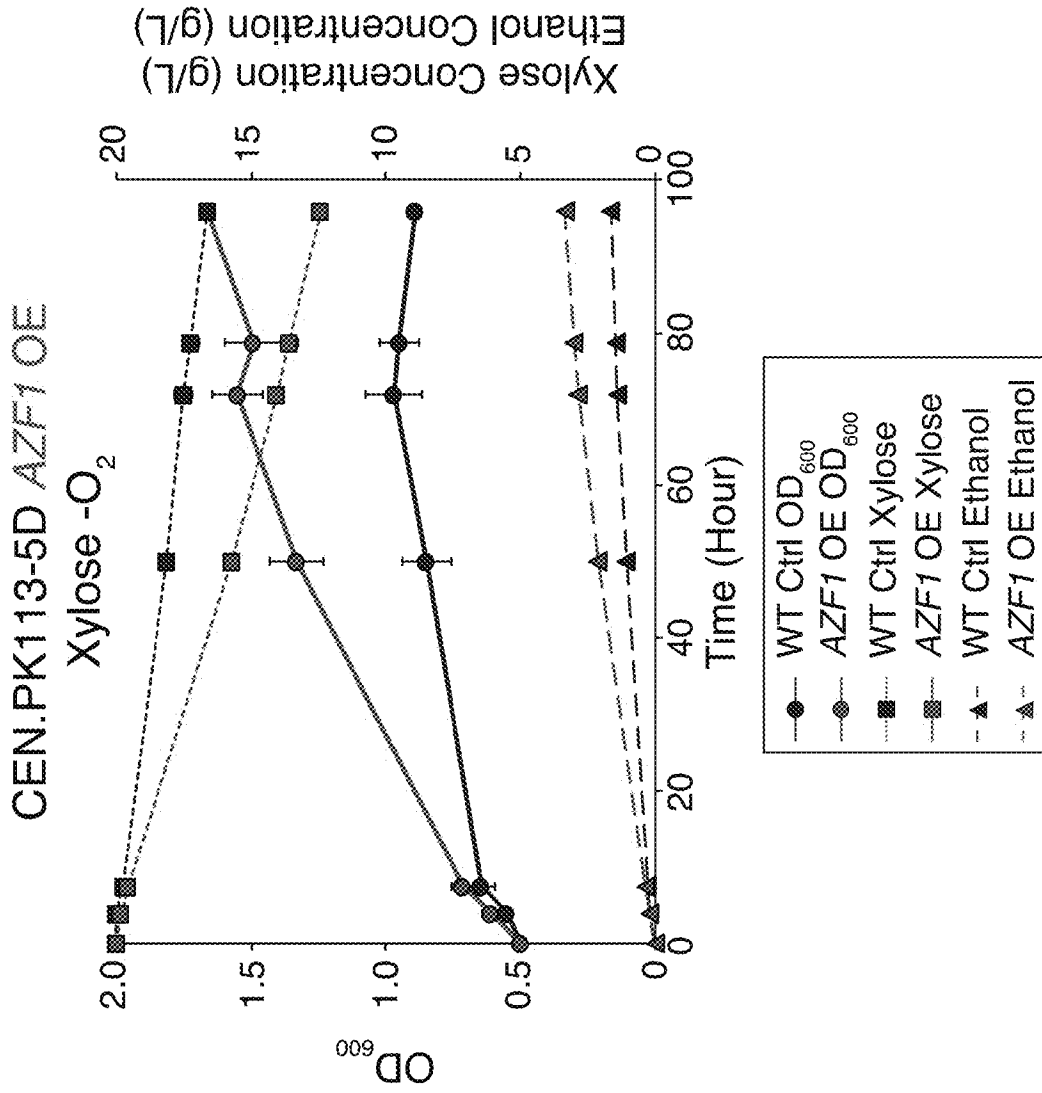


FIG. 8

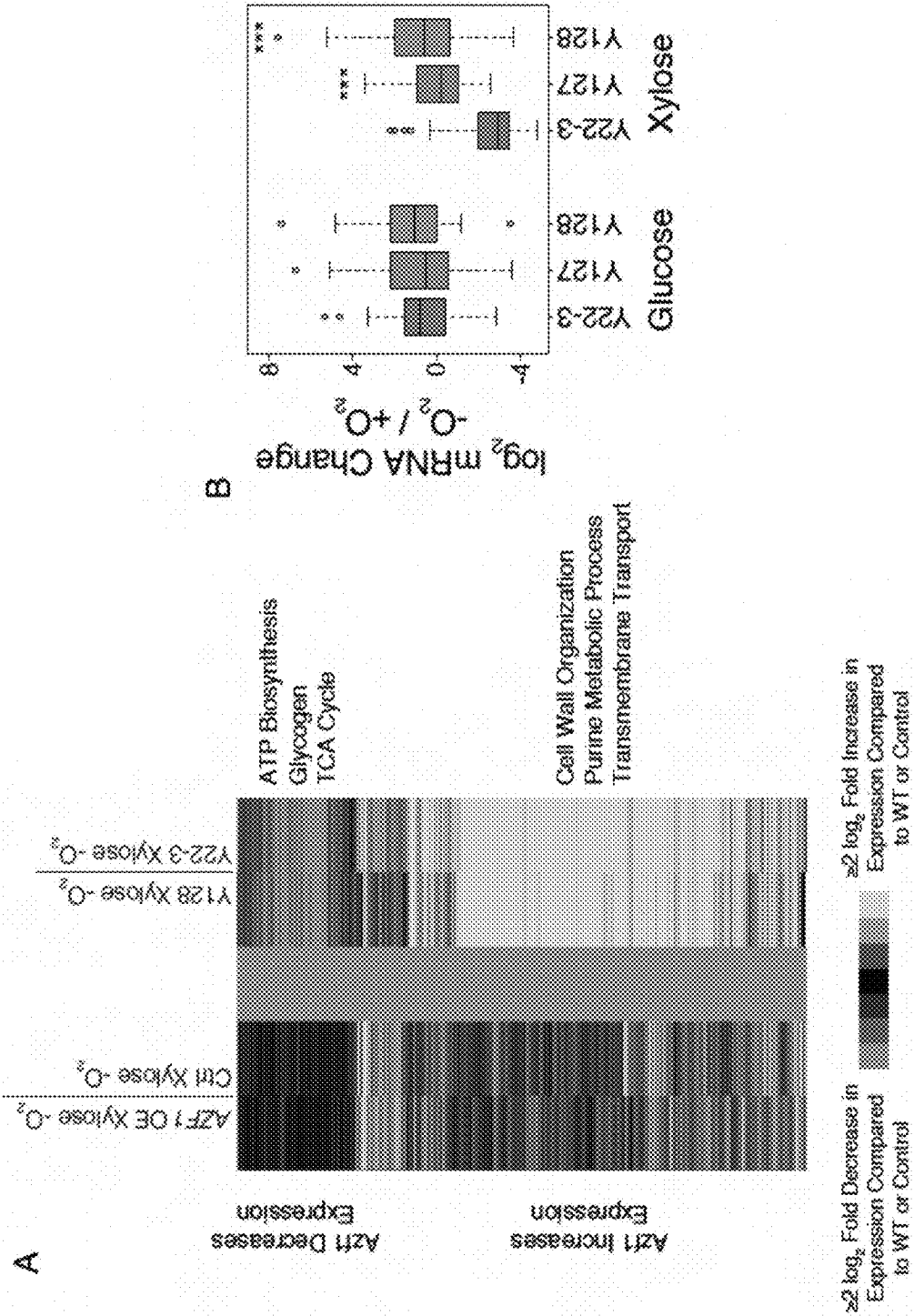


FIG. 9

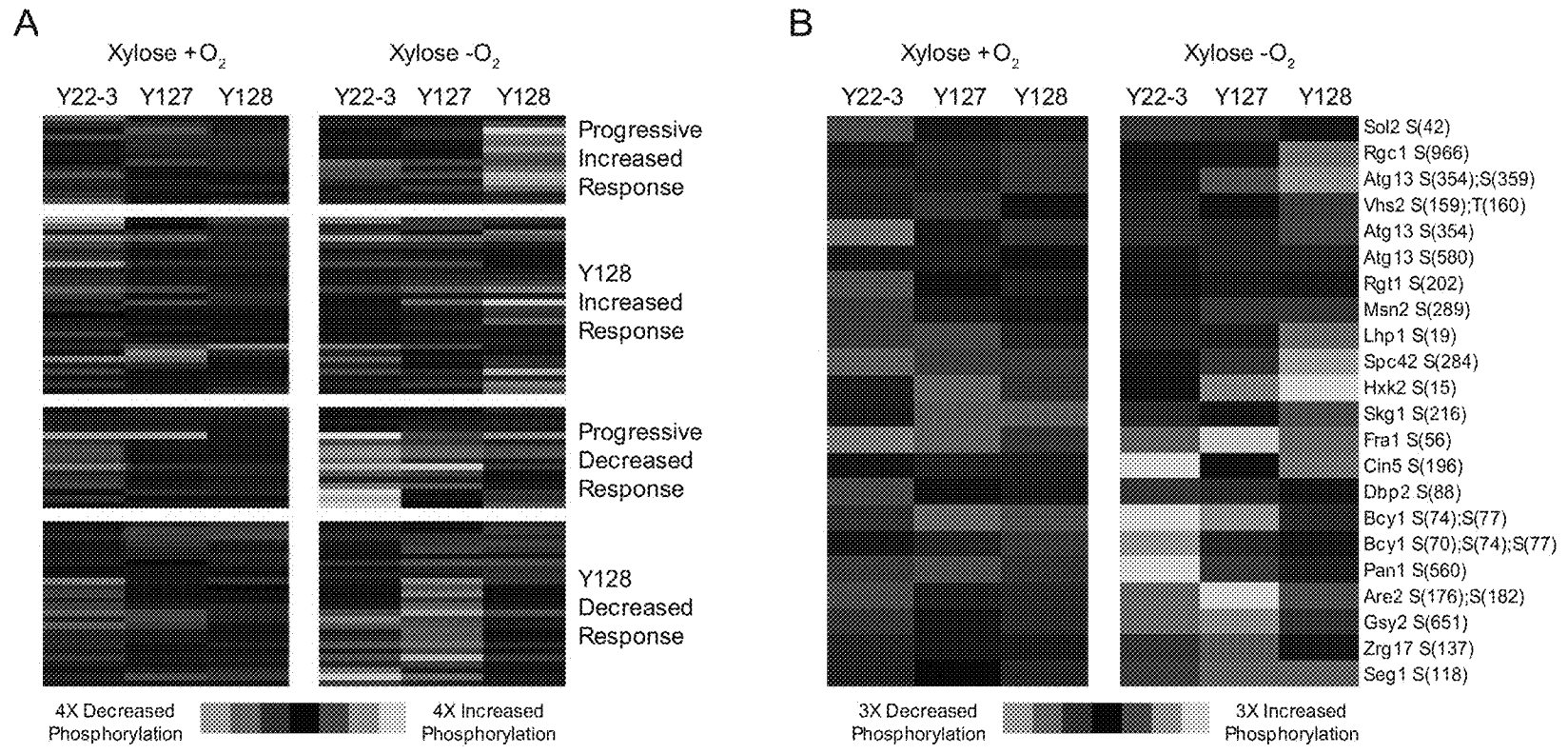


FIG. 10

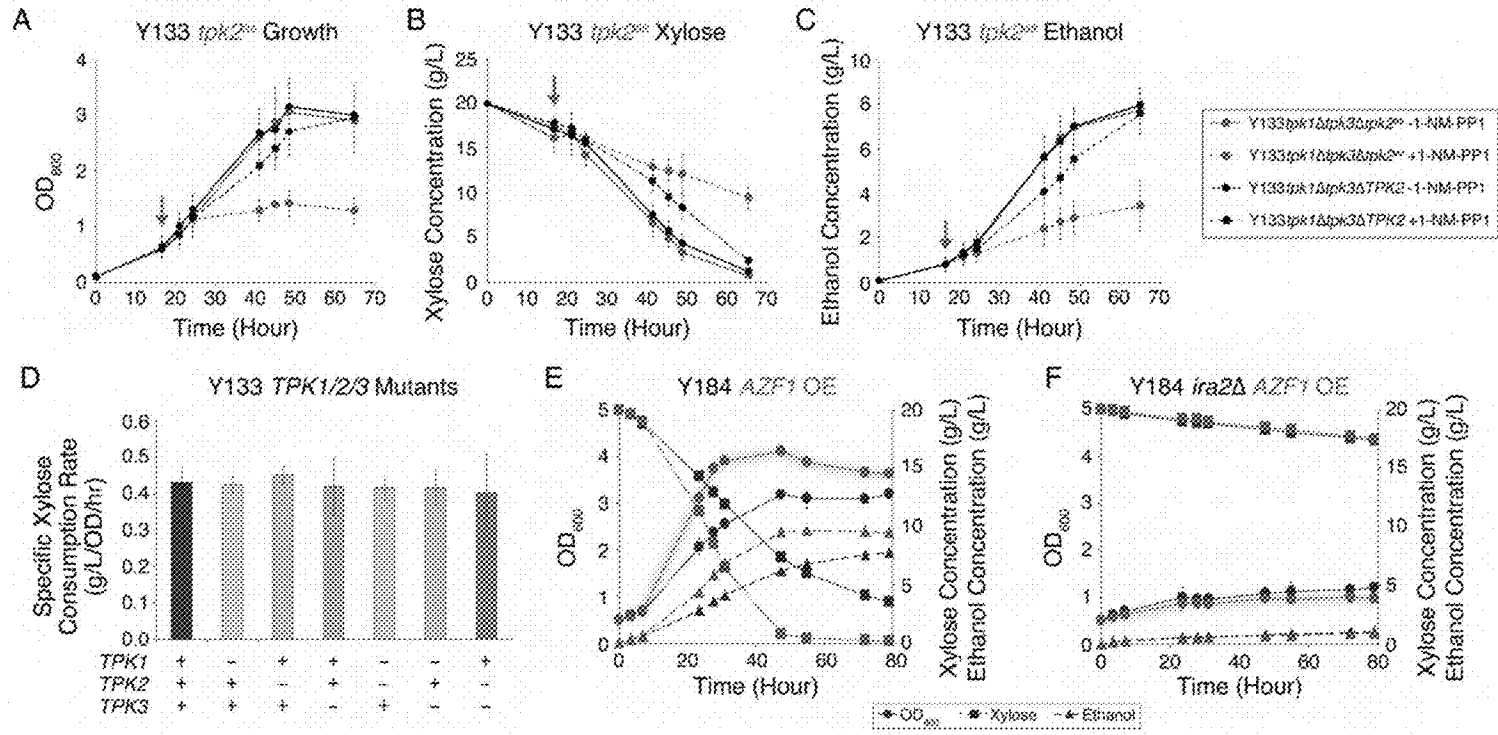


FIG. 11

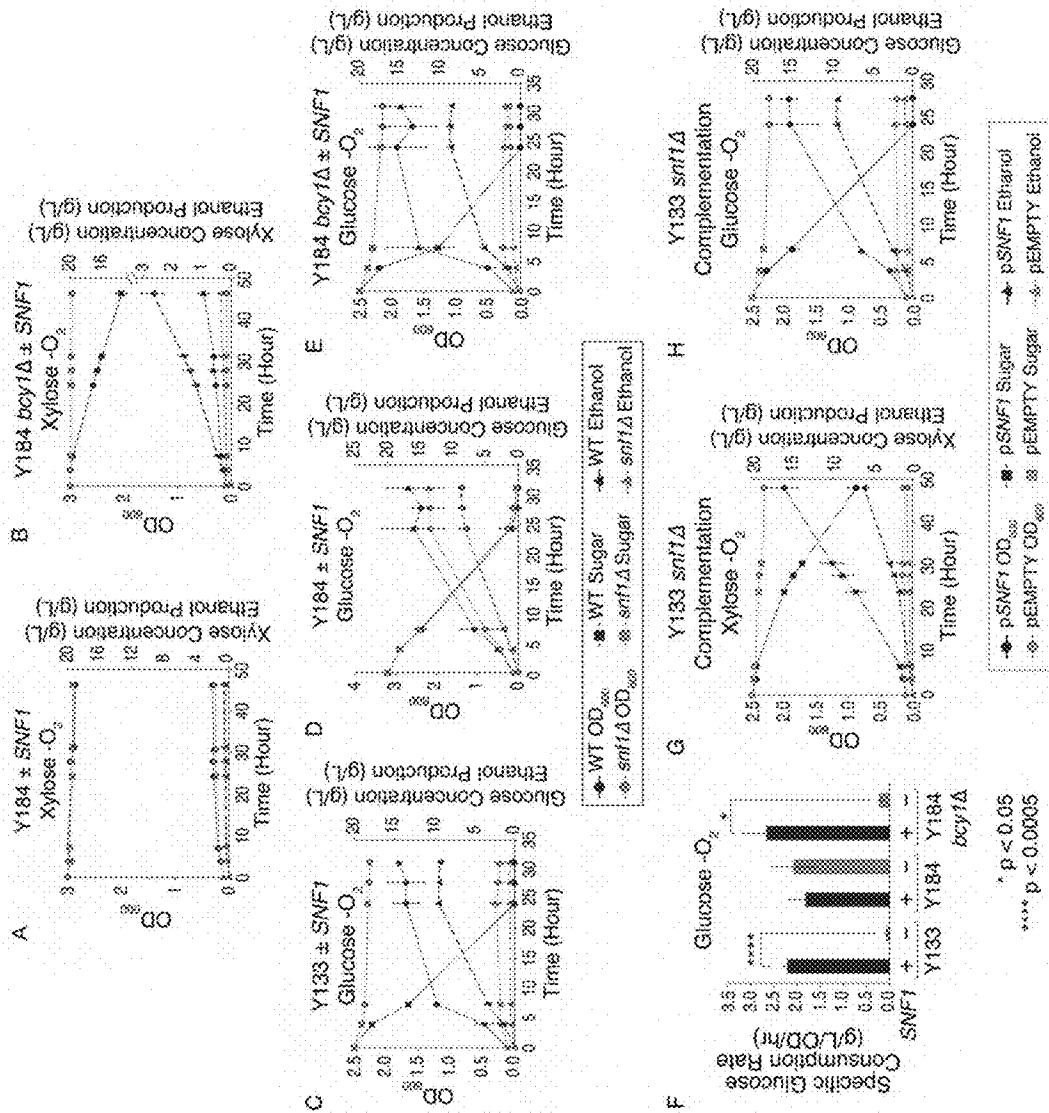


FIG. 12

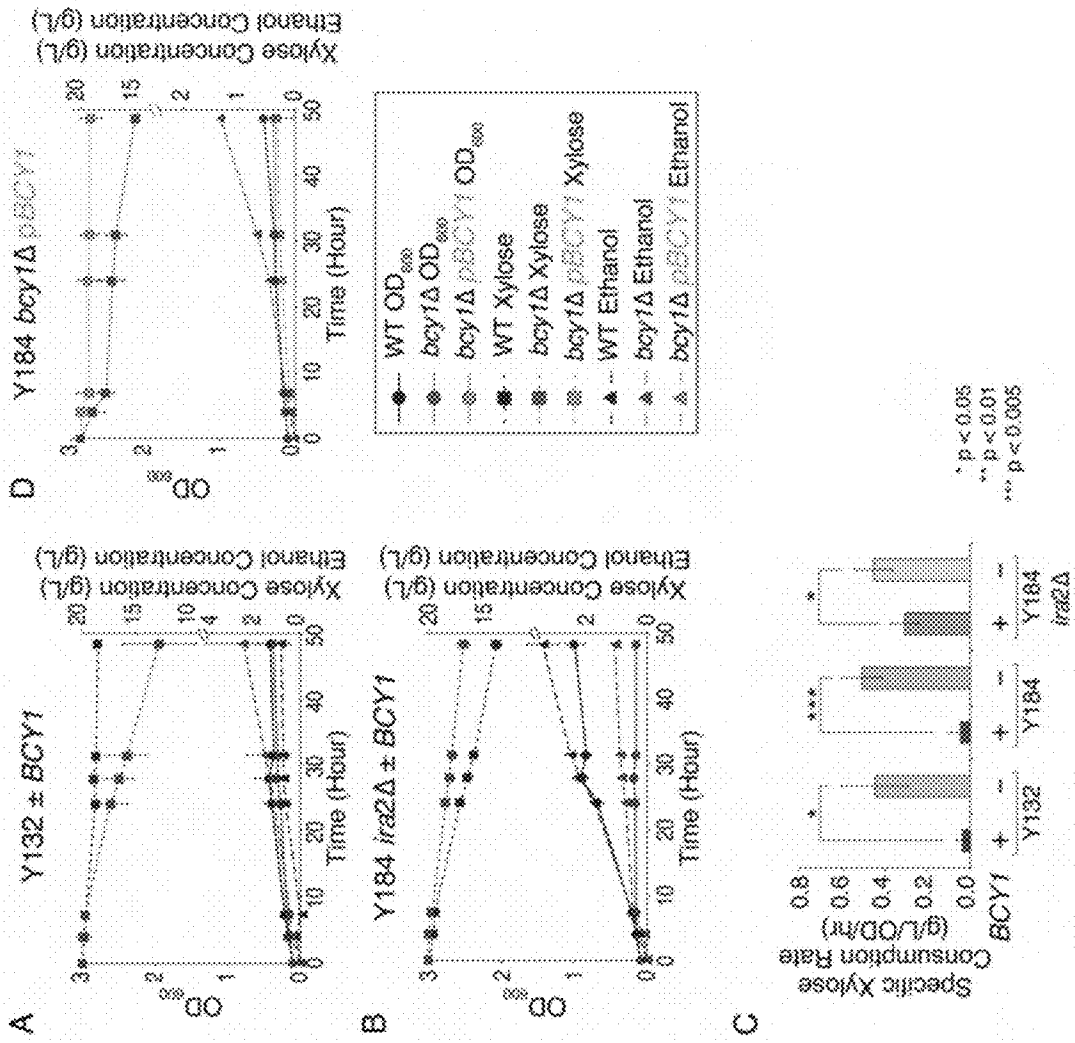


FIG. 13

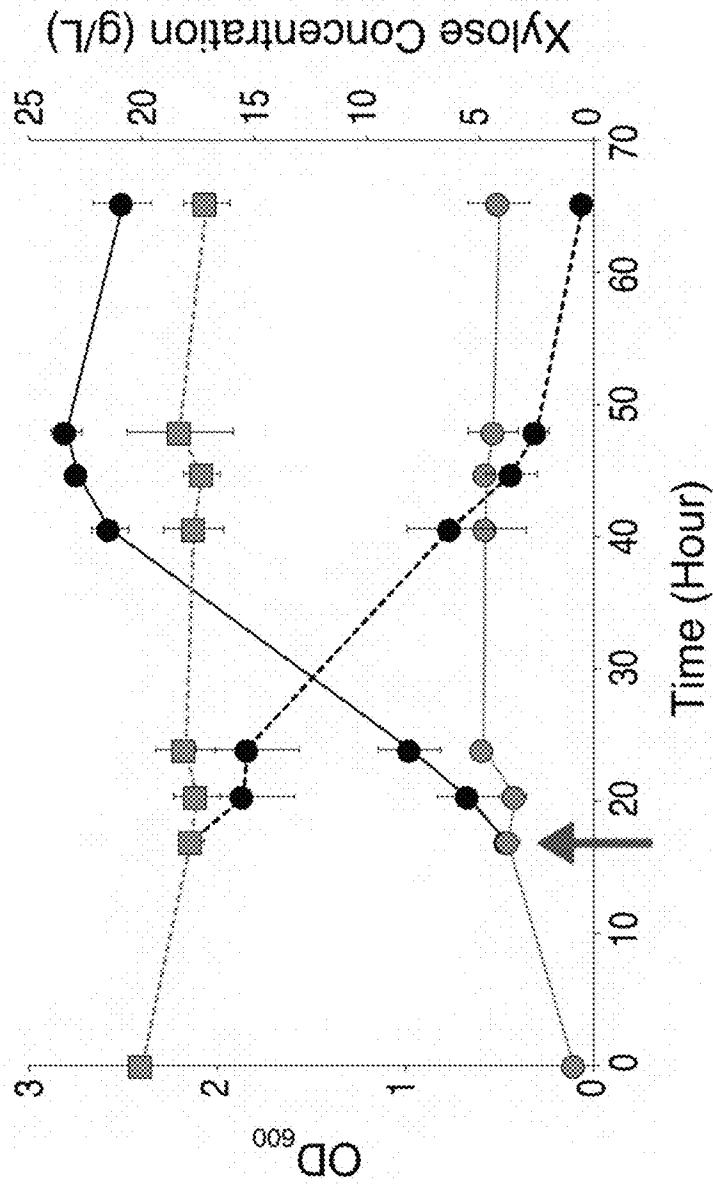


FIG. 14

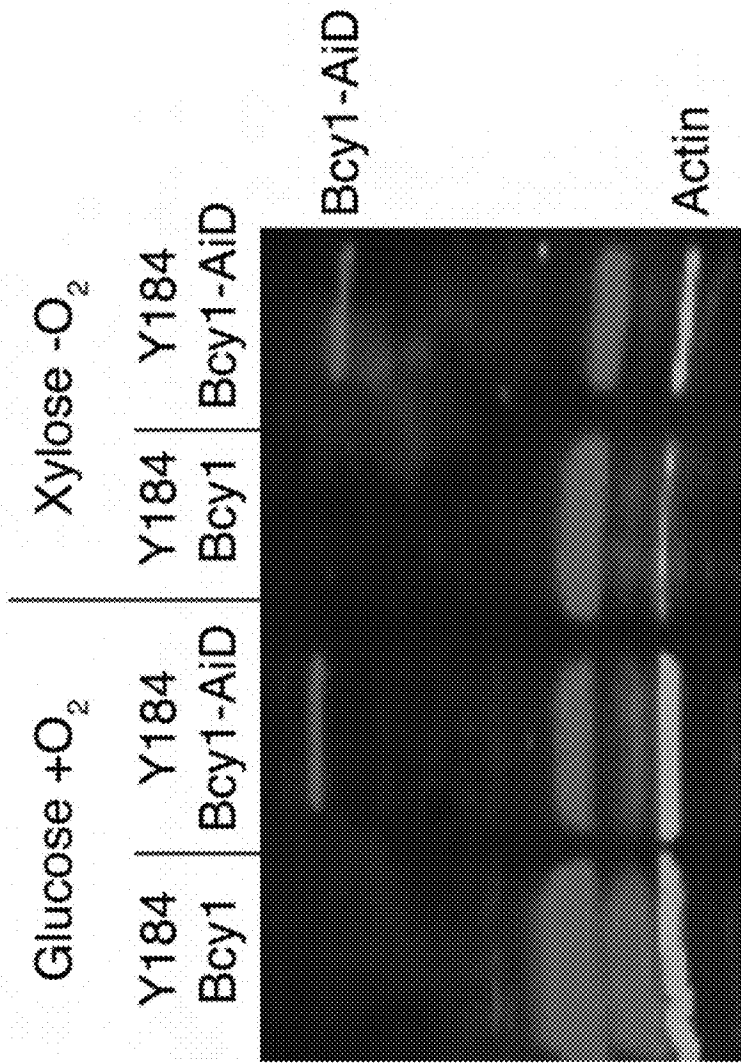


FIG. 15

**ENGINEERED YEAST STRAINS ENABLING
ANAEROBIC XYLOSE FERMENTATION
DECOUPLED FROM MICROBIAL GROWTH**

CROSS-REFERENCE TO RELATED
APPLICATIONS

This application claims the benefit of U.S. Provisional Application No. 62/719,346, filed Aug. 17, 2018, and hereby incorporated by reference.

STATEMENT AS TO RIGHTS TO INVENTIONS
MADE UNDER FEDERALLY SPONSORED
RESEARCH AND DEVELOPMENT

This invention was made with government support under DE-FC02-07ER64494 awarded by the U.S. Department of Energy. The government has certain rights in the invention.

FIELD OF THE INVENTION

The present invention relates to the production of biofuel. More particularly, the present invention relates to rerouting Protein Kinase A (PKA) signaling to control sugar and hypoxia responses to promote anaerobic xylose fermentation in engineered yeast.

BACKGROUND OF THE INVENTION

Cellulosic biomass is a vast source of renewable energy and an abundant substrate for biofuel production. As an alternative to corn-based ethanol, bioethanol can be generated from lignocellulosic (LC) sugars derived from cellulosic biomass of renewable and sustainable plant feedstocks. Energy of cellulosic biomass is primarily stored as the recalcitrant polysaccharide cellulose, which is difficult to hydrolyze because of the highly crystalline structure, and in hemicellulose, which presents challenges because of its structural diversity and complexity. Many microbes cannot natively ferment pentose sugars (e.g., xylose) from complex lignocellulosic biomass, which is composed of cellulose, hemicellulose and lignin fractions. Even when engineered to express the minimal enzymes from native pentose sugar-metabolizing organisms, *S. cerevisiae* cannot ferment xylose from innocuous lab media at industrially-acceptable rates. See Laluce et al., *Applied Microbiol. Biotech.* 166:1908 (2012); Almeida et al., *Biotech. J.* 6:286 (2011), hereby incorporated by reference.

Xylose is a prevalent sugar in both woody and herbaceous plants and a major component of hemicelluloses. Bioconversion of both xylose and glucose is required for the production of cellulosic biofuels. To further complicate matters, plant biomass must be chemically, mechanically, or thermally pretreated prior to enzymatic hydrolysis *ex situ* in order to produce fermentable glucose and xylose monomers. Such pretreatment processes generate a diverse array of degradation products derived from plant cell walls, such as hemicellulose and lignin-derived acetate and aromatic molecules, many of which inhibit cellular metabolism in *S. cerevisiae* and induce microbial stress during hydrolysate fermentation. See Taylor et al., *Biotechnology J.* 7:1169 (2012); Liu, *Applied Microbiol. Biotech.* 90:809 (2011), hereby incorporated by reference. Little is known about how such inhibitors impact xylose fermentation, particularly under strict industrially relevant, anaerobic conditions where ethanol production is maximized.

In view of the current state of the biofuel industry, particularly ethanol production based on glucose- and xylose-containing feedstocks, it can be appreciated that there remains a need for efficient and cost-effective processes for breaking down cellulose and hemicellulose into their constituent sugars.

SUMMARY OF THE INVENTION

The present invention is largely related to the inventors' research efforts to better understand xylose utilization for microbial engineering. The invention relates generally to methods and compositions for digesting lignocellulosic material and more particularly to methods that involve exposing the material to genetically engineered *Saccharomyces cerevisiae* (*S. cerevisiae*).

Based on the inventors' substantial efforts to improve the rate of xylose conversion to ethanol, the present invention provides, in a first aspect, a recombinant yeast genetically engineered to ferment xylose and exhibit a decreased level of BCY1 protein activity, wherein the recombinant yeast provides increased rate of anaerobic xylose fermentation in the yeast relative to a recombinant yeast having the same genetic background but not exhibiting a decreased level of BCY 1 protein activity.

In some embodiments, a degradable tag is operably linked to BCY1 to decrease levels of BCY1 protein activity.

In some embodiments, the recombinant yeast has been genetically engineered to lack BCY1 protein activity by a mutation in the recombinant yeast's BCY1 gene.

In some embodiments, the recombinant yeast exhibits reduced cell growth as compared to a recombinant yeast having the same genetic background but not exhibiting a decreased level of BCY1 protein activity.

In some embodiments, the recombinant yeast is of the genus *Saccharomyces*.

In some embodiments, the recombinant yeast is *Saccharomyces cerevisiae*.

In some embodiments, the yeast produces ethanol at an increased rate relative to a recombinant yeast not exhibiting decreased levels of BCY1 protein activity.

In some embodiments, the increased rate of ethanol production occurs under anaerobic conditions.

In a second aspect, the disclosure encompasses a yeast inoculum, comprising: (a) a recombinant yeast, as described above; and (b) a culture medium.

In a third aspect, the disclosure encompasses a method for producing ethanol by anaerobic fermentation of xylose in yeast, comprising: (a) culturing under ethanol-producing conditions a recombinant yeast, as described above, and (b) isolating ethanol produced by said recombinant yeast.

In a fourth aspect, the disclosure encompasses use of a recombinant yeast, as described above, in the anaerobic fermentation of xylose to produce biofuel.

In a fifth aspect, the disclosure encompasses a recombinant yeast, as described above, for use in the anaerobic fermentation of xylose to produce biofuel.

These and other features, objects, and advantages of the present invention will become better understood from the description that follows. In the description, reference is made to the accompanying drawings, which form a part hereof and in which there is shown by way of illustration, not limitation, embodiments of the invention. The description of preferred embodiments is not intended to limit the invention to cover all modifications, equivalents and alter-

natives. Reference should therefore be made to the claims recited herein for interpreting the scope of the invention.

BRIEF DESCRIPTION OF THE DRAWINGS

The patent or application file contains at least one drawing executed in color. Copies of this patent or patent application publication with color drawing(s) will be provided by the Office upon request and payment of the necessary fee.

FIG. 1 illustrates the response to anaerobiosis in xylose-grown cells. A) Log₂(fold change) in mRNA and protein for cells grown ±O₂, on glucose (black) or xylose (colored), with linear fit (R²) listed. B) Expression of 21 classically defined hypoxic genes (Table 2). Asterisks indicate significant differences in mRNA change relative to Y22-3 (paired T-test). C) Identified promoter element (top) and known Azf1 site (bottom). D) Average (n=3) and standard deviation of xylose utilization rates in marker-rescued (Y133) wild-type ("WT") or strains lacking AZF1 (azf1Δ), over-expressing (OE)AZF1, or harboring an empty vector ("Control") during exponential growth. Xylose utilization rates in marker-rescued Y127 (Y132) empty vector ("Control") and OE of AZF1 are included as indicated. Different growth conditions in the two experiments prevent direct comparison. Asterisks indicate significant differences as indicated (paired T-test).

FIG. 2 illustrates Azf1 and Mga2 regulation of anaerobic xylose responses. A) Average log₂(fold change) in mRNA abundance of denoted genes as listed in the key. B-D) Distributions of log₂(fold change) in mRNA abundances for Hap4 (B), Msn2/Msn4 (C), and Mga2 (D) targets that are affected by AZF1 overexpression and show a corresponding change in Y128 versus controls. Asterisks indicate significant difference compared to azf1Δ versus WT cells (paired T-test). E-F) OD₆₀₀ (circles), xylose concentration (squares), and ethanol concentration (triangles) for strain Y133 (marker-rescued Y128) lacking (mga2Δ, orange plot on the left) or over over-expressing ("OE", green plot on the right) MGA2, and Y133 wild type ("WT") or empty-vector control (black) during anaerobic growth on xylose. Different growth conditions in the two experiments prevent direct comparison.

FIG. 3 illustrates an inferred network regulating phosphorylation changes during anaerobic xylose growth. A) Modules of peptides are shaped and colored according to class (Class A, diamond; Class B, square) and increase (yellow) or decrease (blue) of phosphorylation change across the strain panel, as described in the text. Each module is labeled with the phospho-motif sequence, with small case letter representing the phosphorylated site and "." indicating non-specific residues. Implicated kinase regulators are shown as purple circles; proteins whose peptides belong to each module are shown as smaller circles, color-coded by protein function as listed in the key. Note that proteins with multiple phospho-sites can belong to multiple modules. B) Average (n=3) and standard deviation of the relative in vitro phosphorylation of a PKA substrate for lysates from cells that can (Y128, Y184 bcy1Δ, Y184 Bcy1-AiD) or cannot (Y22-3, Y127) use xylose anaerobically. Orange bars represent phosphorylation in the presence of PKA inhibitor H-89. C) Average (n=3) and standard deviation of sugar utilization rates for Y133 tpk1Δtpk3Δtpk2^{as} or Y133 tpk1Δtpk3ΔTPK2 during anaerobic growth, in the presence (green) or absence (black) of 1-NM-PP1. D) OD₆₀₀ (circles), xylose concentration (squares), and ethanol concentration (triangles) for WT (black) or snf1Δ Y133 (marker-rescued Y128) grown in xylose -O₂. E) Average (n=3) and standard

deviation of xylose utilization rates for strains in the presence (+) or absence (-) of SNF1. Asterisks indicate significant differences according to the key (paired T-tests).

FIG. 4 illustrates mutation of BCY1 decoupling growth from anaerobic xylose metabolism. A) OD₆₀₀ (circles), xylose concentration (squares), and ethanol concentration (triangles) for Y184 (Y22-3 gre3Δisu1Δ) (black) and Y184 bcy1Δ (green) during anaerobic growth on xylose. B-D) Phospho-peptide changes in Y184 bcy1Δ relative to references, for phospho-peptides (rows) specific to Y184 bcy1Δ (B) or similar to Y184 (C) or Y184 ira2Δ (D). Functional enrichments for each denoted cluster are listed below each heat map. (E-F) Growth of strains in glucose+O₂ (E) and xylose-O₂ (F) as indicated in the key. (G-H) Average (n=3) specific xylose consumption (G) or ethanol production (H) rates. Asterisks indicate significant differences relative to Y128 (paired T-test).

FIG. 5 illustrates an integrative model incorporating transcript, phospho-protein, and metabolite changes across the strain panel. Map of central carbon metabolism. Each step is annotated with boxes indicating mRNA difference (left) or phosphorylation difference (middle) in Y128 versus Y22-3, or phosphorylation difference (right) in Y184 bcy1Δ versus Y184 grown anaerobically on xylose, according to the key. Gray indicates no significant change, white represents missing data, and multi-colored blue/yellow boxes indicate multiple phospho-sites with different changes. Metabolites measured previously are colored to indicate an increase (orange) or decrease (magenta) in abundance in Y128 versus Y22-3 grown anaerobically on xylose. Reactions predicted to be active (orange) or suppressed (magenta) in xylose fermenting strains based on mRNA, protein, and/or metabolite abundances are highlighted. Hexose transporters marked with a star have been implicated in xylose transport.

FIG. 6 illustrates proteome and transcriptome response to anaerobic xylose growth across the strain panel. A) Log₂ (fold change) in abundance of Frd1 and Osm1 proteins across all strains and growth conditions in response to anoxia. B) Log₂(fold change) in abundance of ANB1 mRNA across all strains and growth conditions in response to anoxia. C) Log₂(fold change) in mRNA abundance of the 128 genes with a progressive increase anaerobic xylose induction, in Y22-3, Y127, and Y128 growing in glucose±O₂ and xylose±O₂.

FIG. 7 illustrates deletion and over-expression of AZF1 influencing growth and fermentation under anaerobic xylose conditions. A-F) OD₆₀₀ (circles), sugar concentration (squares), and ethanol concentration (triangles) for Y133 (marker-rescued Y128) azf1Δ (red), Y133 AZF1 over-expression ("OE", blue), and Y133 wild type ("WT") or empty-vector control (black) for different sugars and growth conditions as indicated. G) Average (n=3) and standard deviation of sugar utilization rates from each strain during exponential growth. Asterisks indicate significant differences in sugar consumption rates as indicated (paired T-test).

FIG. 8 illustrates AZF1 over-expression increasing xylose fermentation in a second strain background with Y128 mutations. OD₆₀₀ (circles), xylose concentration (squares), and ethanol concentration (triangles) for CEN.PK113-5D with mutations required for xylose metabolism (HOΔ::ScTAL1-Cpxy1A-SsXYL3-loxP-isu1Δhog1Δgre3Δira2Δ7, Table 3) harboring the AZF1 over-expression plasmid (purple) or empty vector control (black).

FIG. 9 illustrates transcriptomic analysis of AZF1 deletion and over-expression during anaerobic xylose fermentation. A) Clustering analysis of log₂(fold change) in mRNA for the 411 genes that show significant (FDR<0.05) effects

in response to over-expression of AZF1 compared to controls and at least a 1.5 fold change in Y128 compared to Y22-3 grown anaerobically on xylose. Enriched functional groups (Bonferroni corrected p -value <0.05) for genes in each cluster are listed on the right. B) Log₂(fold change) in mRNA abundance for genes regulated by Mga2 in Y22-3, Y127, and Y128 cultured in glucose \pm O₂ or xylose \pm O₂. Asterisks indicate expression differences in each strain compared to Y22-3 ($p<0.001$, paired T-test).

FIG. 10 illustrates relative phosphorylation differences for known and inferred PKA targets across the strains growing anaerobically in xylose. Heat map represents relative abundance of phospho-peptides across the panel. Each row represents a phospho-peptide as measured in strains (columns) grown in xylose with (left) and without oxygen (right). Data represent average phospho-peptide abundance relative to the mean abundance across all six data points, such that yellow indicates phospho-peptide abundance above the mean and blue indicates phospho-peptide abundance below the mean, according to the key. A) Shown are all phospho-peptides in FIG. 3A that harbor an RxxS phospho-motif and fall into different categories described in the main text, including Class A (progressive increase/decrease) and Class B (Y128-specific response). B) Shown are 22 sites from panel A that are known PKA target sites identified in the KID database. Protein name and phospho-site(s) are indicated for each row. Notably, some known PKA sites show increases in phosphorylation while others show decreases in phosphorylation in Y128 grown in xylose-O₂.

FIG. 11 illustrates that SNF1 is required for anaerobic xylose fermentation. A-C) OD₆₀₀ (A), xylose concentration (B), and ethanol concentration (C) for Y133tpk1Δtpk3Δtpk2as (blue) or Y133tpk1Δtpk3ΔTPK2 (black) in the presence of 10 μM 1-NM-PP1 (dashed line) or DMSO control (solid line). Timing of 1-NM-PP1 or DMSO addition is indicated by a red arrow. D) Average (n=3) and standard deviation of xylose consumption rates for individual and double TPK knockout strains in Y133. E) OD₆₀₀ (circles), xylose concentration (squares), and ethanol concentration (triangles) for Y184 (Y22-3 gre3Δ isu1Δ)AZF1 over-expression ("OE", purple) or Y184 empty-vector control (black). OD₆₀₀ measurements for Y184 AZF1 OE highlighted in yellow. F) OD₆₀₀ (circles), xylose concentration (squares), and ethanol concentration (triangles) for Y184 ira2Δ AZF1 over-expression ("OE", purple) or Y184 ira2Δ empty-vector control (black). OD₆₀₀ measurements for Y184 ira2Δ AZF1 OE highlighted in yellow.

FIG. 12 illustrates SNF1 is required for anaerobic xylose and glucose fermentation. A-B) OD₆₀₀ (circles), xylose concentration (squares), and ethanol concentration (triangles) for Y184 (Y22-3 gre3Δ isu1Δ) \pm SNF1 (A) and Y184 bcy1Δ \pm SNF1 (B) grown in xylose-O₂. SNF1+strains are plotted in black and snf1Δ strains are plotted in orange. C-E) OD₆₀₀ (circles), glucose concentration (squares), and ethanol concentration (triangles) for Y133 (marker-rescued Y128) (C), Y184 (Y22-3 gre3Δ isu1Δ) \pm SNF1 (D) and Y184 bcy1Δ \pm SNF1 (E) grown in glucose-O₂. SNF1+strains are plotted in black and snf1Δ strains are plotted in orange. F) Average (n=3) and standard deviation of glucose consumption rates for each strain \pm SNF1 during anaerobic growth on glucose. Asterisks indicate significant differences (paired T-test) as indicated. G-H) OD₆₀₀ (circles), sugar concentration (squares), and ethanol concentration (triangles) in Y133 snf1Δ complemented with pSNF1 Moby 2.0 plasmid [101] (black) and pEMPTY control vector [101] (aqua) for cells

grown anaerobically in xylose (G) or glucose (H). The results show that Snf1 is essential for anaerobic xylose fermentation.

FIG. 13 illustrates that deletion of BCY1 influences anaerobic xylose fermentation. A-B) OD₆₀₀ (circles), xylose concentration (squares), and ethanol concentration (triangles) for Y132 (marker-rescued Y127) \pm BCY1 (A) and Y184 ira2Δ \pm BCY1 (B) during growth in xylose-O₂. BCY1+strains are in black and bcy1Δ strains are in green. C) Average (n=3) and standard deviation of sugar utilization rates are shown for each strain \pm BCY1. Asterisks indicate significant differences (paired T-test) as indicated. D) OD₆₀₀ (circles), xylose concentration (squares), and ethanol concentration (triangles) in Y184 bcy1Δ complemented with pBCY1 Moby 2.0 plasmid (aqua) and pEMPTY control vector (green) for cells grown anaerobically in xylose.

FIG. 14 illustrates that inhibition of growth does not promote anaerobic xylose utilization. OD₆₀₀ (circles) and xylose concentration (squares) for Y128 in the absence (black) and presence (green) of 400 mM hydroxyurea, added at the time point indicated by the red arrow, during anaerobic growth on xylose. Addition of hydroxyurea inhibits growth of Y128, but does not promote anaerobic xylose utilization.

FIG. 15 illustrates that Bcy1-AiD is stable in both glucose+O₂ and xylose-O₂. Western blot analysis of Bcy1-AiD using anti-FLAG antibody from cultures grown in glucose+O₂ or xylose-O₂ in Y184 with WT Bcy1 and Y184 with Bcy1-AiD. Anti-actin antibody was used as a loading control.

DETAILED DESCRIPTION OF THE INVENTION

I. IN GENERAL

Before the present materials and methods are described, it is understood that this invention is not limited to the particular methodology, protocols, materials, and reagents described, as these may vary. It is also to be understood that the terminology used herein is for the purpose of describing particular embodiments only, and is not intended to limit the scope of the present invention, which will be limited only by the appended claims.

It must be noted that as used herein and in the appended claims, the singular forms "a", "an", and "the" include plural reference unless the context clearly dictates otherwise. As well, the terms "a" (or "an"), "one or more" and "at least one" can be used interchangeably herein. It is also to be noted that the terms "comprising", "including", and "having" can be used interchangeably.

Unless defined otherwise, all technical and scientific terms used herein have the same meanings as commonly understood by one of ordinary skill in the art to which this invention belongs. Although any methods and materials similar or equivalent to those described herein can be used in the practice or testing of the present invention, the preferred methods and materials are now described. All publications and patents specifically mentioned herein are incorporated by reference for all purposes including describing and disclosing the chemicals, cell lines, vectors, animals, instruments, statistical analysis and methodologies which are reported in the publications which might be used in connection with the invention. All references cited in this specification are to be taken as indicative of the level of skill in the art. Nothing herein is to be construed as an admission that the invention is not entitled to antedate such disclosure by virtue of prior invention.

The practice of the present invention will employ, unless otherwise indicated, conventional techniques of molecular biology, microbiology, recombinant DNA, and immunology, which are within the skill of the art. Such techniques are explained fully in the literature. See, for example, Molecular Cloning A Laboratory Manual, 2nd Ed., ed. by Sambrook, Fritsch and Maniatis (Cold Spring Harbor Laboratory Press: 1989); DNA Cloning, Volumes I and II (D. N. Glover ed., 1985); Oligonucleotide Synthesis (M. J. Gait ed., 1984); Mullis et al. U.S. Pat. No: 4,683,195; Nucleic Acid Hybridization (B. D. Hames & S. J. Higgins eds. 1984); Transcription And Translation (B. D. Hames & S. J. Higgins eds. 1984); Culture Of Animal Cells (R. I. Freshney, Alan R. Liss, Inc., 1987); Immobilized Cells And Enzymes (IRL Press, 1986); B. Perbal, A Practical Guide To Molecular Cloning (1984); the treatise, Methods In Enzymology (Academic Press, Inc., N.Y.); Gene Transfer Vectors For Mammalian Cells (J. H. Miller and M. P. Calos eds., 1987, Cold Spring Harbor Laboratory); Methods In Enzymology, Vols. 154 and 155 (Wu et al. eds.), Immunochemical Methods In Cell And Molecular Biology (Mayer and Walker, eds., Academic Press, London, 1987); and Handbook Of Experimental Immunology, Volumes I-IV (D. M. Weir and C. C. Blackwell, eds., 1986).

"Promoter" refers to a DNA sequence capable of controlling the expression of a coding sequence or functional RNA. In general, a coding sequence is located 3' to a promoter sequence. Promoters may be derived in their entirety from a native gene, or be composed of different elements derived from different promoters found in nature, or even comprise synthetic DNA segments. It is understood by those skilled in the art that different promoters may direct the expression of a gene in different tissues or cell types, or at different stages of development, or in response to different environmental conditions. Promoters that cause a gene to be expressed in most cell types at most times are commonly referred to as "constitutive promoters". Promoters that allow the selective expression of a gene in most cell types are referred to as "inducible promoters".

A "host cell" is a cell which has been transformed or transfected, or is capable of transformation or transfection by an exogenous polynucleotide sequence. A host cell that has been transformed or transfected may be more specifically referred to as a "recombinant host cell". Preferred host cells for use in methods of the invention include yeast cells, particularly yeast cells of the genus *Saccharomyces*, more preferably of the species *Saccharomyces cerevisiae*.

A polypeptide "substantially identical" to a comparative polypeptide varies from the comparative polypeptide, but has at least 80%, preferably at least 85%, more preferably at least 90%, and yet more preferably at least 95% sequence identity at the amino acid level over the complete amino acid sequence, and, in addition, it possesses the ability to increase anaerobic xylose fermentation capabilities of a host yeast cell in which it has been engineered and over-expressed.

The term "substantial sequence homology" refers to DNA or RNA sequences that have de minimus sequence variations from, and retain substantially the same biological functions as the corresponding sequences to which comparison is made.

As used herein, "hybridizes under stringent conditions" is intended to describe conditions for hybridization and washing under which nucleotide sequences that are significantly identical or homologous to each other remain hybridized to each other. Such stringent conditions are known to those skilled in the art and can be found in Current Protocols in Molecular Biology, Ausubel et al., eds., John Wiley & Sons,

Inc. (1995), sections 2, 4 and 6. Additional stringent conditions can be found in Molecular Cloning: A Laboratory Manual, Sambrook et al., Cold Spring Harbor Press, Cold Spring Harbor, N.Y. (1989), chapters 7, 9 and 11. A preferred, non-limiting example of stringent hybridization conditions includes hybridization in 4× sodium chloride/sodium citrate (SSC), at about 65-70° C. (or hybridization in 4×SSC plus 50% formamide at about 42-50° C.) followed by one or more washes in 1×SSC, at about 65-70° C. A preferred, non-limiting example of highly stringent hybridization conditions includes hybridization in 1×SSC, at about 65-70° C. (or hybridization in 4×SSC plus 50% formamide at about 42-50° C.) followed by one or more washes in 0.3×SSC, at about 65-70° C. A preferred, non-limiting example of highly stringent hybridization conditions includes hybridization in 4×SSC, at about 50-60° C. (or alternatively hybridization in 6×SSC plus 50% formamide at about 40-45° C.) followed by one or more washes in 2×SSC, at about 50-60° C. Ranges intermediate to the above-recited values, e.g., at 65-70° C. or at 42-50° C. are also intended to be encompassed by the present invention. SSPE (1×SSPE is 0.15 M NaCl, 10 mM NaH₂PO₄, and 1.25 mM EDTA, pH 7.4) can be substituted for SSC (1×SSPE is 0.15 M NaCl and 15 mM sodium citrate) in the hybridization and wash buffers; washes are performed for 15 minutes each after hybridization is complete. The hybridization temperature for hybrids anticipated to be less than 50 base pairs in length should be 5-10° C. less than the melting temperature (T_m) of the hybrid, where T_m is determined according to the following equations. For hybrids less than 18 base pairs in length, T_m (° C.)=2(# of A+T bases)+4(# of G+C bases). For hybrids between 18 and 49 base pairs in length, T_m (° C.)=81.5+16.6(log₁₀[Na+])+0.41(% G+C)-(600/N), where N is the number of bases in the hybrid, and [Na+] is the concentration of sodium ions in the hybridization buffer ([Na+] for 1×SSC=0.165 M). It will also be recognized by the skilled practitioner that additional reagents may be added to the hybridization and/or wash buffers to decrease non-specific hybridization of nucleic acid molecules to membranes, for example, nitrocellulose or nylon membranes, including but not limited to blocking agents (e.g., BSA or salmon or herring sperm carrier DNA), detergents (e.g., SDS) chelating agents (e.g., EDTA), Ficoll, PVP and the like. When using nylon membranes, in particular, an additional preferred, non-limiting example of stringent hybridization conditions is hybridization in 0.25-0.5M NaH₂PO₄, 7% SDS at about 65° C., followed by one or more washed at 0.02M NaH₂PO₄, 1% SDS at 65° C., see e.g., Church and Gilbert (1984) Proc. Natl. Acad. Sci. USA 81: 1991-1995, (or alternatively 0.2×SSC, 1% SDS).

"Polynucleotide(s)" generally refers to any polyribonucleotide or polydeoxribonucleotide, which may be unmodified RNA or DNA or modified RNA or DNA. "Polynucleotide(s)" include, without limitation, single- and double-stranded DNA, DNA that is a mixture of single- and double-stranded regions or single-, double- and triple-stranded regions, single- and double-stranded RNA, and RNA that is mixture of single- and double-stranded regions, hybrid molecules comprising DNA and RNA that may be single-stranded or, more typically, double-stranded, or triple-stranded regions, or a mixture of single- and double-stranded regions. As used herein, the term "polynucleotide(s)" also includes DNAs or RNAs as described above that contain one or more modified bases. Thus, DNAs or RNAs with backbones modified for stability or for other reasons are "polynucleotide(s)" as that term is intended herein. Moreover, DNAs or RNAs comprising unusual bases, such as inosine, or modified bases, such as tritylated

bases, to name just two examples, are polynucleotides as the term is used herein. It will be appreciated that a great variety of modifications have been made to DNA and RNA that serve many useful purposes known to those of skill in the art. The term “polynucleotide(s)” as it is employed herein embraces such chemically, enzymatically or metabolically modified forms of polynucleotides, as well as the chemical forms of DNA and RNA characteristic of viruses and cells, including, for example, simple and complex cells. “Polynucleotide(s)” also embraces short polynucleotides often referred to as oligonucleotide(s).

The term “isolated nucleic acid” used in the specification and claims means a nucleic acid isolated from its natural environment or prepared using synthetic methods such as those known to one of ordinary skill in the art. Complete purification is not required in either case. The nucleic acids of the invention can be isolated and purified from normally associated material in conventional ways such that in the purified preparation the nucleic acid is the predominant species in the preparation. At the very least, the degree of purification is such that the extraneous material in the preparation does not interfere with use of the nucleic acid of the invention in the manner disclosed herein. The nucleic acid is preferably at least about 85% pure, more preferably at least about 95% pure and most preferably at least about 99% pure.

Further, an isolated nucleic acid has a structure that is not identical to that of any naturally occurring nucleic acid or to that of any fragment of a naturally occurring genomic nucleic acid spanning more than three separate genes. An isolated nucleic acid also includes, without limitation, (a) a nucleic acid having a sequence of a naturally occurring genomic or extrachromosomal nucleic acid molecule but which is not flanked by the coding sequences that flank the sequence in its natural position; (b) a nucleic acid incorporated into a vector or into a prokaryote or eukaryote genome such that the resulting molecule is not identical to any naturally occurring vector or genomic DNA; (c) a separate molecule such as a cDNA, a genomic fragment, a fragment produced by polymerase chain reaction (PCR), or a restriction fragment; and (d) a recombinant nucleotide sequence that is part of a hybrid gene. Specifically excluded from this definition are nucleic acids present in mixtures of clones, e.g., as those occurring in a DNA library such as a cDNA or genomic DNA library. An isolated nucleic acid can be modified or unmodified DNA or RNA, whether fully or partially single-stranded or double-stranded or even triple-stranded. A nucleic acid can be chemically or enzymatically modified and can include so-called non-standard bases such as inosine, as described in a preceding definition.

The term “operably linked” means that the linkage (e.g., DNA segment) between the DNA segments so linked is such that the described effect of one of the linked segments on the other is capable of occurring. “Linked” shall refer to physically adjoined segments and, more broadly, to segments which are spatially contained relative to each other such that the described effect is capable of occurring (e.g., DNA segments may be present on two separate plasmids but contained within a cell such that the described effect is nonetheless achieved). Effecting operable linkages for the various purposes stated herein is well within the skill of those of ordinary skill in the art, particularly with the teaching of the instant specification.

As used herein the term “gene product” shall refer to the biochemical material, either RNA or protein, resulting from expression of a gene.

The term “heterologous” is used for any combination of DNA sequences that is not normally found intimately associated in nature (e.g., a green fluorescent protein (GFP) reporter gene operably linked to a SV40 promoter). A “heterologous gene” shall refer to a gene not naturally present in a host cell (e.g., a luciferase gene present in a retinoblastoma cell line).

As used herein, the term “homolog” refers to a gene related to a second gene by descent from a common ancestral DNA sequence. The term, homolog, may apply to the relationship between genes separated by the event of speciation (i.e., orthologs) or to the relationship between genes separated by the event of genetic duplication (i.e., paralogs). “Orthologs” are genes in different species that evolved from a common ancestral gene by speciation. Normally, orthologs retain the same function in the course of evolution. Identification of orthologs is important for reliable prediction of gene function in newly sequenced genomes. “Paralogs” are genes related by duplication within a genome. Orthologs retain the same function in the course of evolution, whereas paralogs evolve new functions, even if these are related to the original one.

The term “biofuel” refers to a wide range of fuels which are in some way derived from biomass. The term covers solid biomass, liquid fuels and various biogases. For example, bioethanol is an alcohol made by fermenting the sugar components of plant materials and it is produced largely from sugar and starch crops. Cellulosic biomass, such as trees and grasses, are also used as feedstocks for ethanol production and the present invention finds its primary application in this specific field. Of course, ethanol can be used as a fuel for vehicles in its pure form, but it is usually used as a gasoline additive to increase octane and improve vehicle emissions.

“Yeasts” are eukaryotic micro-organisms classified in the kingdom Fungi. Most reproduce asexually by budding, although a few undergo sexual reproduction by meiosis. Yeasts are unicellular, although some species with yeast forms may become multi-cellular through the formation of a string of connected budding cells known as pseudohyphae, or false hyphae, as seen in most molds. Yeasts do not form a single taxonomic or phylogenetic grouping. The term “yeast” is often taken as a synonym for *Saccharomyces cerevisiae*, but the phylogenetic diversity of yeasts is shown by their placement in separate phyla, principally the Ascomycota and the Basidiomycota. The budding yeasts (“true yeasts”) are classified in the order Saccharomycetales.

The nucleotides that occur in the various nucleotide sequences appearing herein have their usual single-letter designations (A, G, T, C or U) used routinely in the art. In the present specification and claims, references to Greek letters may either be written out as alpha, beta, etc. or the corresponding Greek letter symbols (e.g., α , β , etc.) may sometimes be used.

II. THE INVENTION

Engineering microbes for non-native metabolic capabilities is a major goal in strain engineering. Introducing new genes, gene sets, and now complex pathways is relatively facile in modern genetics to imbue strains with novel metabolic capacity. But producing strains that make sufficient quantities of metabolic products remains a major hurdle. The reason likely has less to do with metabolic potential and more to do with how cells regulate activities of enzymes, pathways, and other cellular processes in the context of a cellular system. A better understanding of

cellular regulatory systems that can modulate metabolism without producing undesired off-target effects is an active area research for industrial microbiology.

In the present invention, the inventors used comparative multi-omics and network analysis across the strain panel to understand the mechanism of improved anaerobic xylose flux. The inventors discovered that the parent strain growing anaerobically on xylose but not glucose fails to activate the hypoxic response, whereas evolved strains restore the response, showing that sugar metabolism and oxygen sensing are connected. The inventors found that rewiring cellular signaling by up-regulating Protein Kinase A (PKA) in conjunction with Snf1 activation coordinates a cascade of regulatory events that mediate sugar and hypoxic responses during anaerobic xylose growth. Remarkably, deleting the PKA regulatory subunit decouples division and metabolism by halting growth but promoting rapid anaerobic xylose conversion. This provided an opportunity to distinguish proteome-wide phosphorylation events related to xylose-dependent growth versus fermentation.

The inventors also found that simply fusing the regulatory subunit to a peptide tag combined the disparate benefits of wild-type and mutant strains, improving aerobic glucose growth as well as anaerobic xylose fermentation. Integrating transcriptomic, phosphoproteomic, and metabolomic data revealed a picture of the metabolic logic behind the improved flux of a non-native sugar.

The present invention is a modified yeast strain lacking BCY1 protein activity and capable of anaerobic fermentation of xylose into ethanol without the need for cell growth.

Multi-omic network analysis across strains. The inventors used transcriptomic, proteomic, and phosphoproteomic profiling and bioinformatic analysis to study a series of yeast strains engineered and evolved for different levels of yeast fermentation. Strain Y22-3 is engineered with the minimal genes (xylose isomerase and xylulo-kinase) required for xylose utilization, but cannot use xylose anaerobically. Strain Y127 was evolved in the laboratory from Y22-3, and while it can respire xylose aerobically, it cannot ferment xylose anaerobically. Strain Y128 was evolved from Y127 and is capable of fermenting xylose to ethanol under anaerobic conditions. By comparing multi-omic profiles across these strains, the inventors implicated physiological responses that occur in Y128 but not the other strains to understand the bottlenecks in anaerobic xylose fermentation.

PKA pathway signaling. Phosphoproteomics and signaling network analysis implicated proteins in the PKA pathway as responsible for many changes in phosphorylation in Y128 fermenting xylose anaerobically. To investigate if constitutively active PKA increased anaerobic xylose fermentation, the inventors deleted BCY1, which serves as a regulatory protein turning PKA activity off, in a series of yeast strains known to be able to use xylose as an energy source. They found that in every strain tested, deleting BCY1 inhibited cell growth but enabled cells to consume xylose and produce ethanol anaerobically. In all strains except Y128 (which has additional mutations whose roles are not understood), deletion of BCY1 increased the amount of ethanol produced per yeast cell and per gram of sugar, thereby increasing theoretical yield of ethanol production, and also significantly increased the rate of xylose consumption.

Carbon sensing in yeast. *Saccharomyces cerevisiae* preferentially ferments glucose over other sugars. In the presence of glucose, cells activate glucose utilization genes and repress genes for alternate sugar metabolism, through a regulatory system known as glucose repression. When times

are good, PKA signaling promotes maximal growth and metabolism. PKA is a hetero-tetramer made up of two catalytic subunits (encoded by any of three genes, TPK1, TPK2, TPK3) and two subunits of the regulatory protein BCY1. During times of active growth, the secondary messenger cAMP is produced by adenylate cyclase and binds BCY 1 to inhibit its repressive regulation of the catalytic subunits, allowing TPK1, TPK2, and/or TPK3 to phosphorylate downstream targets. PKA signaling promotes glycolysis, cell growth, and ribosomal protein transcription and represses the stress response, gluconeogenesis, production of carbohydrate storage proteins glycogen and trehalose, and autophagy. While it was previously thought that cAMP binding by BCY 1 led to BCY 1 dissociation, recent work suggests PKA can remain active with BCY 1 still bound, suggesting a more complex regulatory interaction between the catalytic and regulatory subunits. PKA can be activated by at least two upstream branches, including the G-protein coupled receptors and RAS1/RAS2 signaling. IRA2 and its paralog IRA1 are the GTPase-activating proteins that negatively regulate GTP-activated RAS signaling; thus, deletion of IRA2 is expected to up-regulate RAS and, consequently, PKA signaling.

Cells have a complex response when glucose is not available. The absence of glucose alleviates glucose repression, leading to the up-regulation of genes involved in respiration and alternative carbon usage. The resulting energy limitation activates SNF 1, which regulates metabolism of alternate carbon sources (and thus SNF 1 is usually inactive in the presence of glucose). SNF 1 phosphorylates myriad targets, including the glucose-responsive regulators MIG1 and RGT2 and other targets. Together, this results in derepression of gluconeogenic genes, respiratory genes, and genes encoding products allowing the cell to utilize alternative carbon sources in the absence of glucose.

In vegetative cells, PKA and SNF 1 are thought to be active under different situations: PKA is active in the presence of ample nutrients and cellular energy, whereas SNF1 is active during energy limitation due to non-preferred carbon availability. In fact, the kinases are thought to have opposing effects on several shared regulators. For example, the RGT1 transcriptional repressor controls hexokinase 2 (HXK2) transcription; RGT1 phosphorylation by SNF1 activates its repressive effects at the HXK2 promoter, whereas hyperphosphorylation by PKA inhibits RGT1 activity to de-repress this critical regulator of glycolytic flux. Several studies suggest that PKA and SNF1 (or its ortholog in humans, AMPK) can mutually inhibit the other's activity through regulatory feedback that promotes the activity of one pathway or the other. The exception is during pseudohyphal growth, a foraging response seen in some yeast strains and triggered in situations of nitrogen and glucose limitation. Aside of this condition, SNF1 and PKA signaling are thought to be responsive to opposing forces in energy availability.

The following experimental data are provided to illustrate the invention. It is to be understood that a person skilled in the art who is familiar with the methods may use other yeast strains, recombinant vectors, and methodology which can be equally used for the purpose of the present invention. These alterations are included in the scope of the invention.

III. EXAMPLES

In this section, the inventors describe various materials, methods and results related to and supportive of the present invention.

Background and Results

Lignocellulosic plant biomass is a renewable substrate for biofuel production, but many microbes cannot natively use the pentoses that comprise a large fraction of the sugars. Budding yeast *Saccharomyces cerevisiae*, a key microbe in industrial biofuel production, is among the microbes that do not natively recognize xylose as a fermentable sugar, and even when engineered with conversion enzymes strains display low xylose utilization rates. Many studies have attempted to improve xylose metabolism, for example by optimizing xylose metabolism proteins, mutating or over-expressing xylose transporters, inducing genes in the pentose-phosphate pathway, or deleting pathways that siphon intermediates. While these modifications improve the phenotype, many of the individual mutations often do so with relatively small effects. Other studies have used laboratory evolution to select for mutations that enable cell growth on xylose as a sole carbon source, and these approaches have had success. The reason for this defect is not known but is likely regulatory. Under conditions of optimal growth, including on the preferred sugar glucose, yeast promote high activity of Protein Kinase A (PKA) via increased cAMP that inactivates PKA regulatory subunit Bcy1. But in the presence of non-preferred carbon sources that result in low energy availability, cells activate the Snf1 kinase and derepress expression of genes involved in alternate carbon utilization. How to engineer cells to recognize a non-native sugar as fermentable has so far been elusive, especially under anaerobic conditions used by many industrial processes.

To enable anaerobic conversion of xylose to other products, the inventors previously evolved a series of yeast strains: stress-tolerant strain Y22-3 was minimally engineered with xylose isomerase and other genes required for xylose metabolism but was unable to metabolize xylose. This strain was passaged aerobically on xylose-containing

medium to produce the Y127 strain that respire xylose aerobically but cannot use xylose anaerobically. Y127 was thus further evolved without oxygen, generating strain Y128 that can ferment xylose to ethanol anaerobically with yields similar to other engineered strains (Table 1). Null mutations in iron-sulfur cluster scaffold ISU1 and the stress-activated HOG1 kinase enable xylose respiration in Y127, while additional loss of IRA2, an inhibitor of RAS/PKA signaling, and xylitol reductase GRE3 facilitate anaerobic xylose fermentation by Y1287. The IRA2 deletion is interesting, because it is expected to up-regulate RAS and Protein Kinase A (PKA) to promote growth: under optimal conditions, yeast maintain high PKA activity via increased cAMP that inactivates the PKA regulatory subunit Bcy1. The mutations identified in Y128 promote xylose utilization in multiple strain backgrounds, and similar mutations were identified in an independent study, revealing that they have a generalizable impact on strains with the metabolic potential for xylose consumption. Furthermore, mutations in PKA regulators, including IRA2, frequently emerge in laboratory evolution studies that select for improved growth under various conditions. Yet the physiological impacts of these mutations that enable improved phenotypes, in particular anaerobic xylose fermentation, remain unclear.

Multi-omic approaches have been used to characterize alternate sugar metabolism in engineered strains, but distinguishing causal cellular differences from secondary effects is generally a significant challenge. Comparative multi-omics across the strain panel have been used to distinguish transcript, protein, and phospho-protein differences that correlate with, and in several validated cases cause, improved xylose utilization. Integrating these results presents a systems-view of anaerobic xylose fermentation in yeast, which spans many individual responses that improve the phenotype. Our results support that augmenting cellular signaling to remodel many downstream effects that collectively improve the phenotype underlies the benefits in strain Y128. In the process of this work, the inventors present new insights into Snf1 and PKA signaling and the role of PKA mutations in laboratory evolutions.

TABLE 1

Xylose consumption and ethanol production statistics comparing strains from this study to recently reported xylose fermentation strains in the literature.							
1 Strain	2 Culture Conditions	3 Percent Xylose Consumed (Total Time of Xylose Consumption)	4 Total Xylose Consumed (g/L) (Total Time of Xylose Consumption)	5 Total Ethanol Produced (g/L) (Total Time of Xylose Consumption)	6 Xylose Consumption Rate (g/g/hr)	7 Xylose Consumption Rate (g/OD/hr)	8 Ethanol Yield (g/g xylose)
Y128	Anaerobic Batch, YP, 3% Xylose	98% (18 hours)	29.627 ± 0.095 (18 hours)	12.541 ± 0.401 (18 hours)	0.194 ± 0.020	0.249 ± 0.017	0.421 ± 0.014
Y184bcy1A	Anaerobic Batch, YP, 3% Xylose	92% (18 hours)	27.503 ± 1.759 (18 hours)	12.178 ± 0.167 (18 hours)	0.219 ± 0.040	0.263 ± 0.008	0.446 ± 0.006
Y184Bcy1-AiD	Anaerobic Batch, YP, 3% Xylose	99% (18 hours)	29.709 ± 0.290 (18 hours)	12.378 ± 0.290 (18 hours)	0.260 ± 0.021 *	0.334 ± 0.019 *	0.445 ± 0.017
H131-A3-AL ^{cs}	Anaerobic Batch, 2x YNB, 4% Xylose	—	—	—	1.866 +	—	0.41
TMB3422	Anaerobic Batch, 2x YNB, 5% Xylose	—	—	—	0.580 +	—	0.34
TMB3504	Anaerobic Batch, 2x YNB, 5% Xylose	—	—	—	0.760 +	—	0.40

TABLE 1-continued

Xylose consumption and ethanol production statistics comparing strains from this study to recently reported xylose fermentation strains in the literature.							
1 Strain	2 Culture Conditions	3 Percent Xylose Consumed (Total Time of Xylose Consumption)	4 Total Xylose Consumed (g/L) (Total Time of Xylose Consumption)	5 Total Ethanol Produced (g/L) (Total Time of Xylose Consumption)	6 Xylose Consumption Rate (g/g/hr)	7 Xylose Consumption Rate (g/OD/hr)	8 Ethanol Yield (g/g xylose)
SXA-R2P-E	Anaerobic Batch, Synthetic Medium, 4% Xylose	—	—	—	0.98 ⁺	—	0.45
SR8	Anaerobic Batch, YPX, 4% Xylose	—	—	—	0.87 ± 0.02 ⁺	—	0.31 ± 0.05
SR8-fps1A	Anaerobic Batch, YPX, 4% Xylose	—	—	—	0.31 ± 0.02 ⁺	—	0.351 ± 0.001
RWB202-AFX	Anaerobic Batch, Synthetic Medium, 2% Xylose	—	20.627 ± 0.030 (42 hours)	8.306 ± 0.060 (42 hours)	0.34 ⁺	—	0.42
RWB217	Anaerobic Batch, Synthetic Medium, 2% Xylose	—	20.102 ± 0.015 (42 hours)	8.684 ± 0.060 (42 hours)	1.06 ⁺	—	0.43
LVY34.4	Semi-Anaerobic Batch, Synthetic Medium (YPX30), 3% Xylose	—	—	—	1.32 ⁺	—	0.46 ± 0.02
LVY41.5	Semi-Anaerobic Batch, Synthetic Medium (YPX30), 3% Xylose	—	—	—	1.03 ⁺	—	0.45 ± 0.02
BSPX021	Anaerobic Batch, YNB, 2% Xylose	—	17.12 g/L (72 hours)	—	0.217 ± 0.0004 ⁺	—	0.39 ± 0.00
36a(Bvu)	Oxygen Limiting, Synthetic Medium, 4% Xylose	71% (56 hours)	—	11.43 ± 0.02 (56 hours)	0.324 ± 0.008 ⁺	—	0.400 ± 0.001
36a(Xlq)	Oxygen Limiting, Synthetic Medium, 4% Xylose	66% (56 hours)	—	9.64 ± 0.06 (56 hours)	0.241 ± 0.001 ⁺	—	0.465 ± 0.001
36a(TAA)	Oxygen Limiting, Synthetic Medium, 4% Xylose	63% (56 hours)	—	10.15 ± 0.29 (56 hours)	0.333 ± 0.000 ⁺	—	0.400 ± 0.009
36a(HGB5)	Oxygen Limiting, Synthetic Medium, 4% Xylose	77% (56 hours)	—	12.27 ± 0.23 (56 hours)	0.261 ± 0.002 ⁺	—	0.400 ± 0.004
36a(YIT)	Oxygen Limiting, Synthetic Medium, 4% Xylose	64% (56 hours)	—	9.93 ± 0.16 (56 hours)	0.314 ± 0.000 ⁺	—	0.387 ± 0.007

TABLE 1-continued

Xylose consumption and ethanol production statistics comparing strains from this study to recently reported xylose fermentation strains in the literature.							
1 Strain	2 Culture Conditions	3 Percent Xylose Consumed (Total Time of Xylose Consumption)	4 Total Xylose Consumed (g/L) (Total Time of Xylose Consumption)	5 Total Ethanol Produced (g/L) (Total Time of Xylose Consumption)	6 Xylose Consumption Rate (g/g/hr)	7 Xylose Consumption Rate (g/OD/hr)	8 Ethanol Yield (g/g xylose)
39a(Bvu)	Oxygen Limiting, Synthetic Medium, 4% Xylose	92% (56 hours)	—	16.67 ± 0.08 (56 hours)	0.662 ± 0.057 ⁺	—	0.419 ± 0.003
39a(Xlq)	Oxygen Limiting, Synthetic Medium, 4% Xylose	78% (56 hours)	—	13.82 ± 0.98 (56 hours)	0.721 ± 0.045 ⁺	—	0.409 ± 0.014
39a(TAA)	Oxygen Limiting, Synthetic Medium, 4% Xylose	95% (56 hours)	—	16.35 ± 0.34 (56 hours)	0.532 ± 0.011 ⁺	—	0.401 ± 0.006
39a(HGB5)	Oxygen Limiting, Synthetic Medium, 4% Xylose	90% (56 hours)	—	15.63 ± 0.30 (56 hours)	0.704 ± 0.005 ⁺	—	0.402 ± 0.005
39a(YIT)	Oxygen Limiting, Synthetic Medium, 4% Xylose	91% (56 hours)	—	16.27 ± 0.01 (56 hours)	0.586 ± 0.002 ⁺	—	0.412 ± 0.005
MA-B43	Anaerobic Batch, Synthetic SC, 5% Xylose	78% (72 hours)	—	—	—	—	0.33 ± 0.02
DLG-K1T2	Anaerobic Batch, Synthetic SC, 5% Xylose	58% (72 hours)	—	—	—	—	0.37 ± 0.00
DLK-K1T7	Anaerobic Batch, Synthetic SC, 5% Xylose	85% (72 hours)	—	—	—	—	0.38 ± 0.01

Entries marked with “--” indicate reported values were not measured with comparable units.

Column Descriptions:

Column 1	Strain Name
Column 2	Culture Conditions. Calculated from cultures started at an OD of 4.0 (FIG. 4).
Column 3	Percent Xylose Consumed with Total Time of Xylose Consumption in Parentheses
Column 4	Total Xylose Consumed (g/L) with Total Time of Xylose Consumption in Parentheses
Column 5	Total Ethanol Produced (g/L) with Total Time of Xylose Consumption in Parentheses
Column 6	Xylose Consumption Rate (g/g/hr) - Hours 6-16 for Y128, hours 0-18 for bcy1A and Bcy1-AiD
Column 7	Xylose Consumption Rate (g/OD/hr) - Hours 6-16 for Y128, hours 0-18 for bcy1A and Bcy1-AiD
Column 8	Ethanol Yield (g ethanol/g xylose)

In the present invention, the inventors used comparative multi-omics across the strain panel to distinguish transcript, protein, and phospho-protein differences that correlate with improved xylose utilization capabilities, thereby implicating the mechanism of anaerobic xylose fermentation. The inven-

tors first compared the transcriptome and proteome responses of parental strain Y22-3 and evolved strains Y127 and Y128 growing on glucose or xylose, with or without oxygen. Glucose-grown strains showed large changes in mRNA and their encoded proteins when shifted to anaerobiosis, in all three of the strains (FIG. 1A). Surprisingly, however, the strains showed major differences when grown on xylose: Y22-3 shifted to anaerobic conditions showed large changes in mRNA but little change in the encoded proteins (FIG. 1A). Although this strain retained viability during the experiment, its inability to grow anaerobically could have caused a defect in protein production despite major mRNA induction upon the shift. In contrast, strain Y127 was unable to grow yet produced large mRNA changes and moderate changes in the corresponding proteins (FIG. 1A). This included several proteins (e.g. Pdr11 and Anb1) that are not expressed under aerobic conditions but were detected after the anaerobic shift, implicating nascent translation. Nonetheless, the protein changes in xylose-grown Y127 were much smaller than glucose-grown cells shifted to anaerobiosis. In contrast, the correlation between mRNA and protein change was fully recovered in xylose-

grown Y128 shifted to anaerobic growth, on par with the correlation seen in glucose-grown cells (FIG. 1A). Thus, strain Y127 and especially Y22-3 may have a defect in proteome remodeling during anaerobiosis despite large changes in mRNA, specifically when grown on xylose.

The inventors found that Y22-3 and to some extent Y127 showed defective induction of ANB1, a canonical gene in the hypoxic response that is essential for anaerobic translation [40], whereas Y128 showed robust induction of ANB1 (FIG. 6B). While it remains unclear if defective ANB1 induction causes the defect in Y22-3 and Y127 protein accumulation, this observation led the inventors to discover that over 70% of genes classically involved in the hypoxic response (Table 2) were induced at the transcript level in all strains grown on glucose but largely uninduced in xylose-grown Y22-3 and induced progressively stronger in Y127 and Y128, respectively (FIG. 1B). Once again, the differences did not correlate perfectly with growth, since Y127 showed a partial response despite no growth. Furthermore, the defect did not correlate with a lack of transcriptional response, since many other transcripts increased in Y22-3 and Y127 shifted to anaerobic xylose conditions (FIG. 1A). ANB1 Instead, this defect reveals a previously unrecognized connection between the hypoxic response and carbon source in yeast.

TABLE 2

Genes known to be involved in the hypoxic response used to examine the hypoxic response across the strain panel.		
1 Systematic Name	2 Gene Name	3 Description
YBR085W	AAC3	Mitochondrial ADP/ATP translocator
YBR301W	DAN3	Cell wall mannoprotein
YEL047C	FRD1	Fumarate reductase required for anaerobic growth
YEL049W	PAU2	Seripauperin multigene family
YER011W	TIR1	Cell wall mannoprotein
YFL020C	PAU5	Seripauperin multigene family
YHR210C	YHR210C	Putative aldose 1-epimerase protein
YIL011W	TIR3	Cell wall mannoprotein
YIL013C	PDR11	Sterol transporter
YJR047C	ANB1	Anaerobic translation elongation factor eIF-5A
YJR051W	OSM1	Fumarate reductase required for anaerobic growth
YJR150C	DAN1	Cell wall mannoprotein
YJR151C	DAN4	Cell wall mannoprotein
YKL197C	PEX1	AAA-peroxin that recycles peroxisomal targeting receptors under anaerobic conditions
YLL025W	PAU17	Cell wall mannoprotein
YLR037C	PAU23	Cell wall mannoprotein
YML083C	YML083C	Protein of unknown function
YOL161C	PAU20	Seripauperin multigene family
YOR009W	TIR4	Cell wall mannoprotein
YOR010C	TIR2	Putative cell wall mannoprotein
YOR011W	AUS1	Sterol transporter

Column Descriptions:

Column 1	Systematic name for each yeast gene
Column 2	Standard name for each yeast gene, from the <i>Saccharomyces</i> Genome Database
Column 3	Gene functional description for each yeast gene, from the <i>Saccharomyces</i> Genome Database

To further investigate this effect, the inventors identified 128 genes that were induced progressively stronger across the strain panel when shifted to anaerobic xylose conditions, with a pattern similar to the hypoxic response (FIG. 6C).

These were enriched for genes involved in the hypoxic response, ergosterol biosynthesis, cysteine metabolism, and translation ($p < 1 \times 10^{-4}$, hypergeometric test). Promoter analysis identified tandem binding sites of Azf1, a transcription factor (TF) responsive to non-preferred sugars (FIG. 1C). Over half (68) of the 128 progressively induced genes harbored upstream Azf1 motifs ($p = 5.7 \times 10^{-45}$, hypergeometric test), including nearly all of the classical hypoxic genes. Indeed, over-expression of AZF1 increased rates of growth, xylose consumption, and ethanol production in Y128—but only when cells were grown on xylose and anaerobically (FIGS. 1D, 7). In contrast, deletion of AZF1 decreased growth and sugar fermentation, largely specific to anaerobic xylose growth (FIGS. 1D, 7). Although statistically significant, it is notable that the impact of AZF1 was subtle, indicating that it cannot fully explain the improvements in Y128. The Azf1 effect required at least some of the Y128 mutations, as it was observed in a different strain background recapitulating Y128 alleles (FIG. 8) but not in Y22-3.

The inventors identified transcriptome effects of AZF1 deletion or over-expression. AZF1 over-expression in particular had broad effects on the anaerobic-xylose transcriptome, affecting 411 genes ($FDR < 0.05$) whose expression change also paralleled the difference in Y128 compared to Y22-3 grown anaerobically on xylose (FIG. 9A). The set of genes was enriched for those with a match to the Azf1 promoter motif ($p = 3 \times 10^{-2}$, hypergeometric test), supporting the regulatory role of Azf1. Among the affected genes were several TFs and their targets. For example, AZF1 over-expression led to reduced expression of HAP4 that regulates respiration genes as well as stress-responsive MSN2/MSN415, and targets of Hap4 ($p = 1 \times 10^{-3}$, hypergeometric test) and Msn2/Msn4 ($p = 1 \times 10^{-20}$) were enriched among repressed genes (FIG. 2A-2C); deletion of HAP4 and MSN4 were previously shown to improve xylose uptake. AZF1 also reduced expression of the gene encoding Mth1, which interacts with Rgt1 to repress hexose/xylose transporters (FIG. 2A); correspondingly, AZF1 over-expression induced several sugar transporters that can import xylose.

In contrast, AZF1 production induced several targets of the TF Mga2 ($p = 2 \times 10^{-3}$) that responds to hypoxia to regulate genes involved in sterol and fatty acid metabolism (FIG. 2D)—this was intriguing given that defects in the hypoxic response led the inventors to Azf1. To test its importance in anaerobic xylose consumption, the inventors perturbed MGA2 expression directly. Indeed, MGA2 deletion decreased the rate of anaerobic xylose fermentation while MGA2 over-expression improved it (FIG. 2E-2F). These results show that the sugar-responsive Azf1 and the oxygen-responsive Mga2 play important roles in mediating anaerobic xylose fermentation in Y128.

The inventors were especially interested in the upstream regulatory network that mediates the downstream response, including activation of Azf1 and Mga2 targets. The inventors profiled the phosphoproteomes of Y22-3, Y127, and Y128 cultured on xylose with or without oxygen and then applied a novel network approach to infer regulation of strain-specific phosphorylation differences. Because many kinases recognize specific sequences around the phosphorylation site, the inventors identified 'modules' of phosphopeptides that are likely co-regulated and then implicated kinases and phosphatases that may control their phosphorylation change. First, the inventors grouped peptides based on their changes in phosphorylation when each strain was shifted from aerobic to anaerobic xylose conditions, identifying peptides with progressive phosphorylation increases

or decreases across the strain panel (“Class A” increases or decreases) and peptides with responses uniquely higher or lower in Y128 (“Class B” increases or decreases). Next, the inventors partitioned each group into ‘modules’ of peptides that harbor similar sequences around the phosphorylated site (‘phospho-motifs’). Module peptides therefore share the same phosphorylation pattern and similar phospho-motifs, and thus are enriched for peptides that are likely co-regulated. Reasoning that module peptides are regulated by the same upstream regulator(s), the inventors then searched a background network of protein interactions for proteins that physically interact with more module peptides than expected by chance (FDR<0.05). The inventors focused on kinases whose phosphorylation preference matches the module phospho-motif, thereby implicating those kinases as direct regulators of module peptides.

The resulting network implicated several regulators in the anaerobic xylose response (FIG. 3A). Peptides that showed highest phosphorylation levels in Y22-3 upon anaerobic xylose shift included ribosomal proteins and translation factors, whose modules were associated with PKA subunit Tpk2 and Cka1 of the CK2 kinase, which phosphorylates translation factors in other organisms to modulate translation. Other modules showed increased phosphorylation in Y128 shifted to anaerobic xylose conditions, including those connected to cyclin-dependent kinase Cdc28 that regulates carbon-metabolism enzymes and proteins required for division.

The inventors were intrigued by multiple modules connected to PKA subunits Tpk1 and Tpk2, since mutations in IRA2 are predicted to up-regulate RAS/PKA signaling. Two PKA-associated modules showed reduced phosphorylation in Y128, spanning translation factors described above—indeed, the proteins whose peptides belong to these two modules are enriched for known targets of PKA ($p=3\times 10^{-3}$), implicating the other peptides as potential PKA targets. But two other modules of peptides showed increased phosphorylation in xylose-grown Y128 shifted to anaerobic conditions (FIG. 3A). These modules included known PKA targets and phospho-sites (FIG. 10) such as hexokinase 2 that promotes glycolytic flux and stress-responsive TF Msn2 that is inhibited by PKA phosphorylation. Intriguingly, this module also included hypoxia-responsive Mga2 at a site that matches the known PKA specificity. MGA2 genetically interacts with IRA2 in high-throughput datasets, supporting a link between PKA and MGA2 function. Furthermore, Mga2 targets are significantly up-regulated in Y128 that lacks functional IRA2 compared to nonfermenting strains (FIG. 9B). Together, these results suggest that signaling through PKA is modulated in Y128.

Indeed, further experiments verified the importance of PKA signaling. First, lysate from Y128 grown anaerobically on xylose showed increased phosphorylation of a PKA substrate in vitro compared to the other two strains, which was blocked by PKA inhibitor H-89 (FIG. 3B). Second, Y128 harboring a single analog-sensitive allele of PKA subunits (*tpk2^{as}*) required PKA function for both growth on and fermentation of xylose: inhibition of *tpk2^{as}* activity via addition of the inhibitor 1-NM-PP1 rapidly inhibited growth and fermentation during anaerobic xylose utilization (FIG. 3C, 11). Third, the beneficial effects of AZF1 over-expression required deletion of IRA2 (FIG. 11E and 11F). Together, these results show that RAS/PKA activity is required for anaerobic xylose fermentation in Y128, even though some proteins known to be regulated by PKA show decreased phosphorylation in these conditions (FIG. 10B and below).

One of the Tpk2-connected modules of phosphorylated peptides was also associated with the Snf1 kinase, which is activated by low cellular energy to induce alternative-carbon utilization genes. This was interesting, because PKA and Snf1 are not normally active under the same conditions—the two regulators can produce antagonistic effects and even inhibit each other’s activity. To test this network prediction, the inventors knocked out SNF1 from Y128 and measured xylose fermentation capabilities. Indeed, SNF1 is essential (but insufficient) in the absence of other Y128 mutations) for anaerobic xylose utilization in Y128 (FIG. 3D-3E, 13). Thus, PKA activity and SNF1 are required for the effect, validating the network predictions.

Deletion of IRA2 upregulates PKA as well as other downstream effects of RAS. To distinguish if inducing PKA alone is enough to mediate the response, the inventors deleted the PKA negative regulatory subunit BCY1 in strain Y184 (Y22-3 *gre3Δ isu1Δ*) that can use xylose aerobically but not anaerobically. Y184 lacking BCY1 could not grow anaerobically on xylose, as seen for other non-preferred carbon sources—but surprisingly the cells rapidly fermented xylose despite growth arrest, at rates and ethanol yields surpassing other published xylose-converting strains (FIG. 4A, 14, Table 1). Xylose fermentation by the Y184 *bcy1Δ* was associated with increased PKA activity, since lysate from Y184 *bcy1Δ* cells grown anaerobically on xylose showed increased phosphorylation of a PKA target that was blocked by the H-89 PKA inhibitor (FIG. 3B). Thus, up-regulating PKA activity through BCY1 deletion enabled rapid xylose fermentation but in the absence of growth.

The unique phenotype of the Y184 *bcy1Δ* strain provided an opportunity to distinguish phosphorylation events related to growth versus metabolism. Phosphorylation patterns shared between Y184 and Y184 *bcy1Δ*, neither of which can grow anaerobically on xylose, are therefore associated with growth arrest; in contrast, phosphorylation patterns common to Y184 *bcy1Δ* and Y184 *ira2Δ*, which share the ability to ferment xylose anaerobically but differ in growth capabilities, are implicated in xylose metabolism (FIG. 4B-4D). The 210 peptides whose phosphorylation levels were unique to Y184 *bcy1Δ* or shared between non-growing strains occurred on proteins involved in translation, ribosome biogenesis, nucleotide biosynthesis (including ribonucleotide reductase *Rnr2*), and DNA replication—all functions required for division. Many of these phosphorylation patterns are likely an indirect consequence of arrest. To test if growth arrest via direct inhibition of *Rnr2* could block growth but enable fermentation, the inventors used the RNR inhibitor hydroxyurea to arrest growth; but this treatment also halted xylose utilization (FIG. 14).

In contrast, many of the 335 phosphorylation patterns unique to Y184 *bcy1Δ* or shared between the two xylose-fermenting strains were linked to metabolism, including on hexose transporters *Hxt2* and *Hxt6* that influence xylose uptake, enzymes involved in glycolysis (*Plk2*, *Fbp26*, *Tdh1/2*, *Cdc19*, *Pda1*, *Pdc1*), trehalose biosynthesis that regulates glycolytic overflow (*Tsl1*, *Tps2*, *Tps3*, *Nth2*), and glycerol and alcohol dehydrogenases that recycle NADH during high glycolytic flux (*Gpd1*, *Gut1*, *Adh1*). Augmentation of proteins in these pathways have been implicated in improved xylose utilization.

Several phosphorylation patterns implicated in Y128 (FIG. 3A) were not recapitulated in the Y184 *bcy1Δ* strain, suggesting that they are not strictly required for anaerobic xylose fermentation. For example, unlike Y128, phosphorylation of known *Cdc28* targets was reduced in Y184 *bcy1Δ* compared to Y184 *ira2Δ*, strongly suggesting that *Cdc28*-

dependent phosphorylation in Y128 is linked to division and not xylose metabolism. Despite increased PKA signaling in the *bcy1Δ* strain (FIG. 3B), several of the known and predicted PKA phosphorylation sites in Y128 showed reduced phosphorylation upon BCY1 deletion. For example, relative to Y128, Y184 *bcy1Δ* showed decreased phosphorylation of serine 15 (S15) on the main hexokinase, HXK2, whose phosphorylation normally increases activity. Finally, the Y184 *bcy1Δ* strain displayed several unique phosphorylation patterns not observed in the other strains. Remarkably, this included decreased phosphorylation on Hog1 activating site T174, a phenotype seen when Hog1 activity is reduced. This suggests that effects of BCY1 deletion mimic Hog1 inactivation that enhances xylose consumption, and raises the possibility that PKA activity can suppress Hog1 activation.

Although BCY1 deletion enhances anaerobic xylose metabolism, it slows aerobic growth on glucose, which is a problem for industrial propagation of microbial cells. As a proof-of-principle for industrial use, the inventors therefore generated a tagged version of Bcy1 in attempt to enable auxin-dependent degradation and made an important discovery: simply fusing a peptide to the carboxyl-terminus of Bcy1 (without enabling degradation) was enough to combine the benefits of BCY1+ and *bcy1Δ* strains in aerobic and anaerobic conditions, respectively (FIG. 4E-H). When grown aerobically on glucose to mimic industrial propagation, cells expressing a Bcy1-AID fusion (but without auxin-regulated controllers) grew to higher cell titers than Y128, consistent with functional Bcy1 activity (FIG. 4E). But when shifted at high density to anaerobic xylose conditions, the strain dramatically reduced growth and rapidly fermented xylose to ethanol, mimicking the *bcy1Δ* strain (FIG. 4F-4H, Table 1). The Bcy1 protein fusion remained readily detectible by Western blot, indicating that the recapitulation of the *bcy1Δ* phenotype was not through Bcy1 degradation (FIG. 16). These results and our network analysis raise the possibility of more subtle modulation of PKA activity than simple up-regulation.

The inventors' results provide new insight into the upstream regulatory network that enables anaerobic xylose fermentation and the downstream cellular responses that mediate it. *S. cerevisiae* engineered with the required metabolic enzymes remains unable to utilize xylose without further modification, indicating a bottleneck in regulation rather than metabolic potential. This bottleneck blocks metabolism but also prevents the hypoxic response, revealing for the first time a connection between sugar and oxygen sensing in yeast. Evolved strain Y128 activates PKA signaling while requiring Snf1 for anaerobic xylose usage, leading to a cascade of downstream effects that involve the sugar-responsive Azf1, oxygen-responsive Mga2, and downstream effectors that control respiration (Hap4), stress response (Msn2/Msn4), and sugar transport (Mthl) among others. Integrating transcriptomic, phosphoproteomic, and metabolomic data across the strain panel provides a glimpse of the downstream cellular response (FIG. 5), with combined effects including induction of sugar transporters, up-regulation of genes and metabolites in the non-oxidative branch of the pentose phosphate pathway, increased abundance of xylolytic and glycolytic intermediates, reduced abundance of overflow metabolites, and sharp reduction in respiration components. The results support previous metabolic engineering studies that suggested the need for widespread cellular remodeling, in addition to individual metabolic changes, for optimal product production.

Many of the downstream responses identified have been implicated before in improved xylose fermentation, including over-expression of xylose transporters, pentose-phos-

phate pathway enzymes, modulation of hexokinase, and down-regulated stress-activated transcription factors. However, in many prior studies, alteration of individual genes through deletion or over-expression often has only minor effects on the phenotype. This is also consistent with our results: although the inventors validated predictions to show that Azf1 and Mga2 contribute to anaerobic xylose fermentation, their individual effects are small compared to the impact of upstream regulatory changes. Thus, the improvement seen in Y128 compared to its progenitors emerges from the combined effects of many downstream changes that collectively impact the phenotype. This is also consistent with the literature showing that combinatorial gene mutation produces additive or epistatic effects. For example, Papatridis et al. tested the effects of individual gene deletions on co-fermentation of glucose and xylose; the most significant benefits emerge when multiple genes were combined, e.g. co-deletion of hexokinase HXK2 and ubiquitin ligase RSP5. Over-expression of transaldolase (TAL1) or glyceraldehyde-3-phosphate dehydrogenase (GDP1), or deletion of phosphatase PHO13 or glucose-6-phosphate dehydrogenase (ZWF1), all impact xylose fermentation individually, but combinatorial effects emerge from combining TAL1 induction and PHO13 deletion or GDP1 over-expression with ZWF1 ablation. Predicting which combinatorial modifications to make is likely to be a significant challenge going forward, especially for mutations outside of known metabolic pathways. It is in this light that selecting for regulatory changes through laboratory evolution studies can produce combinatorial effects of large combined impact.

The benefits in Y128 emerge in part through co-activation of PKA along with Snf1. Snf1 is required for growth on non-preferred carbon sources, and thus its involvement in xylose utilization does not seem surprising. However, Snf1 alone is not sufficient to enable anaerobic xylose fermentation unless IRA2 or BCY1 are also deleted (FIGS. 3D-3E). The response to xylose in anaerobically-grown Y128 thus combines responses normally seen on poor carbon sources (i.e. Snf1 activation, induced expression of hexose transporters including some that transport xylose, altered hexokinase regulation, and Azf1 activation) with responses typically restricted to the presence of abundant glucose (i.e. phosphorylation events associated with increased glycolytic flux, reduced expression of respiration and stress-responsive genes, and active PKA signaling). Surprisingly, Snf1 is specifically required for anaerobic growth, on both xylose and glucose, in the context of Y128 mutations. The link of Snf1 to anaerobic growth has not been reported to our knowledge, although Snf1 has recently been tied to oxygen responses: glucose-grown yeast exposed to hypoxia phase-separate glycolytic enzymes in a Snf1-dependent manner, in a process influenced by Ira2. Snf1 and PKA are not normally coactivated in yeast. The primary exception is during invasive growth, a foraging response in which starved cells invade a solid substrate. Invasive growth is driven by combined PKA and Snf1 activation, which is triggered by nitrogen and glucose limitation. This ecological response may explain the link between sugar and oxygen responses, since cells undergoing substrate invasion may prepare for impending hypoxia.

Numerous laboratory evolution studies selecting for improved growth identified mutations in PKA signaling, including in strains evolved under sugar and nitrogen limitation, continuous growth in rich medium, growth on non-preferred carbon sources, and on industrial wort. These studies often identify mutations in RAS and RAS regulators, adenylate cyclase that generates cAMP, and especially IRA2. IRA2 mutations have also been implicated as frequent second site suppressors of other mutations to enable improved growth. Yet mutations in BCY1 are not generally

identified in laboratory evolutions. This may reveal an important link: that while up-regulating RAS improves growth, which is the primary selection in most laboratory evolution studies, up-regulating PKA by Bcy1 deletion can have important effects including on industrially relevant traits that could be missed by growth-based assays. It will be important to dissect the different physiological effects of increased PKA activity via RAS up-regulation (i.e. IRA2 deletion) or PKA modulation directly via BCY1 deletion.

At the same time, the inventors' results strongly suggest that PKA is not simply up-regulated but rather 'rewired' to target some peptides while disfavoring others. This could emerge from differential activation of phosphatases, but could also occur if PKA is being directed to different sets of targets (perhaps through differential composition of PKA via the three Tpk subunits). Bcy1 is thought to direct PKA to specific sets of targets, much like AKAP proteins in mammalian cells. The inventors' results that a Bcy1 peptide fusion (Bcy1-AiD) combines the benefits of BCY1+ cells in aerobic glucose medium and bcy1Δ cells in anaerobic xylose suggest a complex interplay. Recent studies in mammalian cells reveal that the PKA regulatory subunit does not dissociate from catalytic PKA subunits upon cAMP binding, raising the possibility that structural differences in Bcy1-AID could direct PKA to different sets of proteins. That some well-characterized PKA phospho-sites are up-regulated while others are suppressed in anaerobically-grown Y128 supports this hypothesis. Furthermore, how these changes impact other traits important to industrial conditions—including stresses of complex lignocellulosic plant material, high mixed sugar concentrations, and alternate nutrient availability, will be important considerations.

Integrating transcriptomic, phosphoproteomic, and metabolomic data across the strain panel also presents the downstream logic of anaerobic xylose fermentation (FIG. 5). Transcriptomic and metabolomic data are easiest to interpret, and the combined effects in Y128 lead to induction of sugar transporters as well as genes and metabolites in the non-oxidative branch of the pentose phosphate pathway, increased abundance of xylolytic and glycolytic intermediates, reduced abundance of overflow metabolites, and sharp reduction in respiration components. Phosphorylation changes remain difficult to interpret in isolation, but the inventors propose that the integrative model shown in FIG. 5 can be used to predict the functions of corresponding phosphorylation changes and may have utility in future engineering strategies. The inventors' study demonstrates the power of integrative and comparative strategies to dissect cellular responses of an important industrial trait.

Example 2

Materials and Methods

Media and Growth Conditions. Cells were grown in YP medium (10 g/L yeast extract, 20 g/L peptone) with glucose, xylose, or galactose added at 20 g/L final concentration,

unless otherwise noted. Antibiotics were added where indicated at the following concentrations: 200 mg/L G418, 300 mg/L Hygromycin B, 100 mg/L ClonNat. For aerobic growth, cultures were grown at 30° C. with vigorous shaking in flasks. For anaerobic growth, media was incubated at 30° C. in a Coy anaerobic chamber (10% CO₂, 10% H₂, and 80% N₂) for ≥16 hours before inoculation, and cultures were grown at 30° C. in flasks using stir bars spinning at 300 rpm to reduce flocculation. Cultures were inoculated with a saturated culture of cells grown in YP-glucose medium, washed one time with the desired growth media, at the specified OD₆₀₀ value as indicated. Cell growth was measured using OD₆₀₀, and extracellular sugar and ethanol concentrations were measured with HPLC-RID (Refractive Index Detector) analysis.

Strain and Cloning. *Saccharomyces cerevisiae* strains used in this study are described in Table 3. The creation of Y22-3, Y127, and Y128 and their antibiotic marker-rescued counterparts with the KanMX gene was removed (Y36, Y132, and Y133, respectively) was described previously⁷. All strains express the minimal required genes for xylose metabolism, including xylose isomerase (xylA from *Clostridium phytofermentans*), xylose kinase (XYL3 from *Scheffersomyces stipites*), and transaldolase (TAL3 from *S. cerevisiae*). Gene knockouts were generated by homologous recombination of the KanMX or Hph cassettes into the locus of interest and verified using multiple diagnostic PCRs. AZF1 and MGA2 were over-expressed using the MoBY 2.0 plasmid and empty vector as a control, growing cells in medium containing G418 to maintain the plasmid. BCY1 was deleted from indicated strains through homologous recombination of the KanMX cassette and verified by multiple diagnostic PCRs. Strain Y184 harboring integrated BCY1/-AiD (Auxin-induced-Degron) was generated as follows: all plasmids were provided by National BioResource Program (NBRP) of the Ministry of Education, Culture, Sports and Technology (MEXT), Japan. Plasmid pST1933 (NBRP ID BYP8880) containing 3x Mini-AiD sequences, 5x FLAG Tag and KanMX was modified to include the 329 bp of BYC1 3' UTR between the 5x FLAG tag and the KanMX marker gene. This construct (3x Mini-AiD, 5x FLAG tag, BCY1 3' UTR, and KanMX) was amplified and inserted downstream and in-frame of BYC1 in Y184 (Y22-3 gre3Δisu1Δ) to form strain Y184 Bcy1-AiD. The integrated construct was verified by sequencing. Neither the pTIR plasmid enabling auxin-dependent degradation nor auxin was required for the desired effect (not shown), thus these were omitted from the analysis. Phenotypes introduced by BCY1 deletion were complemented by introducing BCY1 on a CEN plasmid: to generate the plasmid, BCY1 and 1000 bp upstream and 1000 bp downstream were amplified from Y128 and inserted into a NatMX-marked CEN plasmid via homologous recombination and sequence verified. This plasmid or the empty vector (pEMPTY) were transformed into appropriate strains. Phenotypes resulting from SNF1 deletion were complemented using the SNF1 MoBY 2.0 plasmid and compared to the empty vector control.

TABLE 3

Strains used in this study.	
1 Strain Name	2 Description
Y22-3	CRB Strain with xylose utilization genes (G418 ^R)
Y127	Evolved Y22-3 for aerobic xylose utilization (G418 ^R)
Y128	Evolved Y127 for anaerobic xylose utilization (G418 ^R)
Y36	Y22-3 marker-rescued (MR) - lacking KanMX cassette
Y132	Y127 marker-rescued (MR) - lacking KanMX cassette

TABLE 3-continued

Strains used in this study.	
1 Strain Name	2 Description
Y133	Y128 marker-rescued (MR) - lacking KanMX cassette
Y133 azf1Δ	Y133 azf1Δ::KanMX (G418 ^R)
Y133 AZF1	Y133 containing AZF1-MoBY 2.0 Plasmid (G418 ^R)
MoBY Y133	Y133 containing Empty Vector MoBY 2.0 Plasmid (G418 ^R)
MoBY Control	
CEN.PK1 13-5D	CEN.PK113-5D with HOA::ScTAL1-CpxylA-SsXYL3-loxP, isu1Δ::loxP, hog1Δ::kanMX, gre3Δ::loxP, ira2Δ::loxP
Xylose Strain	
CEN.PK1 13-5D	CEN.PK113-5D Xylose Strain containing AZF1-MoBY 2.0 Plasmid (G418 ^R)
Xylose Strain	
AZF1 MoBY	
CEN.PK1 13-5D	CEN.PK113-5D Xylose Strain containing Empty Vector MoBY 2.0 Plasmid (G418 ^R)
Xylose Strain	
MoBY Control	
Y184	Y22-3 gre3Δ::MR isu1Δ::loxP-Hyg (Hyg ^R)
Y243	Y22-3 gre3Δ::MR isu1Δ::loxP-Hyg ira2Δ::MR (Hyg ^R)
Y132	Y132 bcy1Δ::KanMX (G418 ^R)
bcy1Δ	
Y184	Y22-3 gre3Δ::MR isu1Δ::loxP-Hyg bcy1Δ::KanMX (Hyg ^R , G418 ^R)
bcy1Δ	
Y243	Y22-3 gre3Δ::MR isu1Δ::loxP-Hyg ira2Δ::MR bcy1Δ::KanMX (Hyg ^R , G418 ^R)
bcy1Δ	
Y133	Y133 SNF1::Hyg (Hyg ^R)
snf1Δ	
Y184	Y22-3 gre3Δ::MR isu1Δ::loxP-Hyg snf1Δ::NatMX (Hyg ^R , Nat ^R)
snf1Δ	
Y184	Y22-3 gre3Δ::MR isu1Δ::loxP-Hyg bcy1Δ::KanMX snf1Δ::NatMX (Hyg ^R , G418 ^R , Nat ^R)
bcy1Δsnf1Δ	
Y243	Y22-3 gre3Δ::MR isu1Δ::loxP-Hyg ira2Δ::MR snf1Δ::NatMX (Hyg ^R , Nat ^R)
snf1Δ	
Y243	Y22-3 gre3Δ::MR isu1Δ::loxP-Hyg ira2Δ::MR bcy1Δ::KanMX snf1Δ::NatMX (Hyg ^R , G418 ^R , Nat ^R)
bcy1Δsnf1Δ	
Y133	Y133 snf1Δ::Hyg containing SNF1Δ-MoBY 2.0 Plasmid (Hyg ^R , G418 ^R)
snf1Δ	
SNF1 MoBY	
Y133	Y133 snf1Δ::Hyg containing Empty Vector MoBY 2.0 Plasmid (Hyg ^R , G418 ^R)
snf1Δ MoBY	
Control	
Y133	Y133 mga2Δ::KanMX (G418 ^R)
mga2Δ	
Y133	Y133 containing MGA2-MoBY 2.0 Plasmid (G418 ^R)
MGA2 MoBY	
Y184	Y22-3 gre3Δ::MR isu1Δ::loxP-Hyg bcy1Δ::KanMX containing pBCY1 CEN Plasmid (Hyg ^R , G418 ^R , Nat ^R)
bcy1Δ	
pBCY1	
Y184	Y22-3 gre3Δ::MR isu1Δ::loxP-Hyg bcy1Δ::KanMX containing empty vector CEN Plasmid (Hyg ^R , G418 ^R , Nat ^R)
bcy1Δ	
Empty Control	
Y132	Y132 BCY1-3' AiD tag (3x Mini-Auxin Induced Degron Sequence-5x FLAG-BCY1-3' UTR- KanMX) (G418 ^R)
BCY1-3' AiD	
Y184	Y22-3 gre3Δisu1Δ BCY1-3' AiD tag (3x Mini-Auxin Induced Degron Sequence-5x FLAG- BCY1-3' UTR-KanMX) (G418 ^R)
BCY1-3' AiD	
Y243	Y36 gre3Δisu1Δira2Δ BCY1-3' AiD tag (3x Mini-Auxin Induced Degron Sequence-5x FLAG-BCY1-3' UTR-KanMX) (G418 ^R)
BCY1-3' AiD	

Column Descriptions:

Column 1	Strain Name
Column 2	Description of Strain Used

Y133 *tpk1Δtpk3Δtpk2^{as}* was generated using CRISPR/Cas9-mediated genome editing. TPK1 and TPK3 were deleted in Y133 independently and verified by PCR. sgRNA sequence (GTGATGGATTATATCAGAAGG) that targeted the location within TPK2 to be replaced was cloned into the pXIPHOS vector using NotI (GenBank accession MG897154), which contains the constitutive RNR2 promoter driving the Cas9 gene and NatMX resistance gene, using gapped plasmid repair using HiFi DNA Assembly Master Mix from NEB. *tpk2as* repair templates were generated by PCR of the whole ORF of *tpk2as* from a strain containing mutants of the TPK genes that are sensitive to the ATP-analogue inhibitor 1-NM-PP1 (TPK1 M164G, TPK2 M147G, TPK3 M165G). Purified repair templates were co-transformed at a 20-fold molar excess with the pXIPHOS-TPK2 sgRNA plasmid into Y133 *tpk1Δtpk3Δ* strain. Colonies resistant to nourseothricin were restreaked onto YPD two times to remove the plasmid (and were verified to now be sensitive to nourseothricin) and *tpk2as* presence was verified by sequencing. Y133 *tpk1Δtpk3Δtpk2^{as}* was grown in xylose anaerobically for 17 hours at which point 10 μM 1-NM-PP1 or DMSO control was added to the cultures.

Transcriptomic sample collection, library construction, and sequencing. Y22-3, Y127, and Y128 grown in YPD or YPX, with or without oxygen, were collected in biological duplicate on different days. Data from replicates were highly correlated (average R^2 of $\log_2(\text{fold changes})=0.93$) and additional statistical power was incurred by analyzing across all strain data. Duplicates were used due to limitations with phosphoproteomic techniques (see below). Cultures were inoculated from a saturated aerobic sample grown in rich glucose medium (YPD), washed with the corresponding growth media, and grown for ~3 generations aerobically or anaerobically until the cultures reached mid-log phase (OD_{600} of ~0.5). Strains Y22-3 and Y127 were inoculated in rich xylose medium (YPX) at an OD_{600} of ~0.5 and incubated anaerobically for the same amount of time as the other cultures. Y22-3 and Y127 retained over 95% viability as measured by CFU/mL after 17 hours of anaerobic incubation on xylose. Growth was halted by adding 30 mL of culture to ice cold 3.75 mL 5% phenol (pH<5)/95% ethanol solution, cultures were spun for 3 min at 3000 rpm, the decanted pellet was flash frozen in liquid nitrogen and stored at -80° C. until needed. Total RNA was isolated by hot phenol lysis and DNA was digested using Turbo-DNase (Life Technologies, Carlsbad, Calif.) for 30 min at 37° C., followed by RNA precipitation at -20° C. in 2.5 M LiCl for 30 min. rRNA depletion was performed using EpiCentre Ribo-Zero Magnetic Gold Kit (Yeast) RevA kit (Illumina Inc, San Diego, Calif.) and purified using Agencourt RNACleanXP (Beckman Coulter, Indianapolis, Ind.) following manufacturers' protocols. RNA-seq library generation was performed using the Illumina TruSeq stranded total RNA kit (Illumina) using the sample preparation guide (revision C) with minor modifications, AMPure XP bead for PCR purification (Beckman Coulter, Indianapolis, Ind.), and SuperScript II reverse transcriptase (Invitrogen, Carlsbad, Calif.) as described in the Illumina kit. Libraries were standardized to 2 μM. Cluster generation was performed using standard Cluster kits (version 3) and the Illumina Cluster station. Single-end 100-bp reads were generated using standard SBS chemistry (version

3) on an Illumina HiSeq 2000 sequencer. All raw data were deposited in the NIH GEO database under project number GSE92908.

Y133, Y133 *azf1Δ*, Y133 with the AZF1 MoBY 2.0 plasmid, and Y133 carrying the MoBY 2.0 empty-vector control were grown in xylose-O₂ (+/-G418 as needed), duplicate samples were collected on different days and RNA was isolated and DNA digested as described above. The inventors focused on genes affected in multiple strains for increased statistical power. rRNA depletion was performed using EpiCentre Ribo-Zero Magnetic Gold Kit (Yeast) RevA kit (Illumina) following manufacturer's protocols and cleaned using Qiagen RNease MinElute Cleanup kit (Qiagen, Hilden, Germany). RNA-seq library generation was performed using the EpiCentre Strand Specific ScriptSeq Kit (Illumina) as above except that Axygen AxyPrep Mag PCR Clean-up Kits for PCR purification (Axygen, Corning, N.Y.) were used and LM-PCR was performed using 12 cycles using EpiCentre ScriptSeq Index PCR Primers (Illumina) and Epicenter Failsafe PCR Enzyme Mix (Illumina). Single-end 100-bp reads were generated using standard SBS chemistry (version 4) on an Illumina HiSeq 2500 sequencer and the two FASTQ files for each sample were combined using the "cat" command.

RNA-seq processing and analysis. Reads for all RNA-seq experiments were processed with Trimmomatic version 0.351 and mapped to the Y22-3 genome using Bowtie 2 version 2.2.2 with default settings. HTSeq version 0.6.054 was used to calculate read counts for each gene using the Y22-3 annotation. Differential expression analysis was performed using edgeR version 3.6.8 using pairwise comparisons, taking Benjamini and Hochberg false discovery rate (FDR)<0.05 as significant. Raw sequences were normalized using the reads per kilobase per million mapped reads (RPKM) method. Clustering analysis was performed using MClust version 4.457 and visualized using Java TreeView (<http://jtreeview.sourceforge.net>). Functional enrichment analysis was performed using the FunSpec database or a hypergeometric test using GO annotation terms (downloaded 2017-10-18). All examined targets of TFs were obtained from YeasTract using only those with DNA binding evidence.

AZFI motif identification. The inventors analyzed the $\log_2(\text{fold change})$ in expression for each strain grown anaerobically in xylose compared to anaerobically in glucose. Genes with a progressive xylose-responsive induction across the strain panel were identified if the replicate-averaged $\log_2(\text{fold-change})$ in Y127 was >1.5 fold higher than in Y22-3, and if the replicate-averaged $\log_2(\text{fold-change})$ in Y128 was also ≥ 1.5 fold higher than in Y127. 21 classical hypoxic genes, those known to be involved in the hypoxic response, were selected from the literature to measure the hypoxic response (Table 2) and for enrichment analysis to score the hypoxic response. The inventors selected 15 of these genes with no induction in Y22-3 grown anaerobically on xylose and performed motif analysis, by extracting 1000 bp upstream of these genes and submitting to MEME using the 'any number of sequences' model. The top motif matched the *Azf1* binding site in TomTom. WebLogo was used to construct the final PWM logos for publication. Matches to this matrix were identified in 500 bp upstream regions in the Y22-3 genome using MAST with default settings. A total of 433 significant (E-value<10) sites were identified in all intergenic regions in the genome.

Analysis of expression in *azf1Δ* and AZFI-over-expressing strains. Differentially expressed genes were identified using edgeR as described above, comparing Y133 *azf1Δ* to

Y133 (identifying 441 differentially expressed genes at FDR<0.05) and comparing Y133 AZF1-MoBY 2.0 compared to Y133 carrying the empty vector control (1,525 genes at FDR<0.05). The inventors identified 411 genes whose expression was significantly altered (FDR<0.05) by AZF1 over-expression and whose replicate-averaged expression was at least 1.5× different in Y128 versus Y22-3 cultured anaerobically on xylose and whose expression showed the same directionality as in response to AZF1 over-expression. That is, genes that showed an increase in expression when AZF 1 was over-expressed (relative to the control) also showed an increase in expression in Y128 (relative to Y22-3), and vice versa. Functional enrichment analysis was performed using the FunSpec database or hypergeometric test of GO annotation terms (downloaded 2017-10-18) or compiled sets of TF targets.

Label Free Quantitative Proteomics Preparation and Analysis. For comparison of the Y22-3, Y127, and 128 proteomes, duplicate samples were collected from the same samples used for RNA-seq above. Duplicates were used due to limitations with phosphoproteomic techniques (see below). 35 mL of cultures were spun for 3 min at 3000 rpm, the supernatant was removed and the pellet was flash frozen in liquid nitrogen and stored at -80° C.

Label free proteomics were performed similarly to previous work. For protein extraction and digestion, yeast cell pellets were lysed by glass bead milling (Retsch GmbH, Germany). Lysate protein concentration was measured via bicinchoninic acid protein assay (Thermo Pierce, Rockford, Ill.), and yeast proteins were reduced through incubation in 5mM dithiothreitol (DTT) for 45 minutes at 58° C. Free cysteines were alkylated in 15 mM iodoacetamide in the dark for 30 minutes. The alkylation was stopped with 5 mM DTT. A 1 mg protein aliquot was digested overnight at room temperature in 1.5 M urea with trypsin (Promega, Madison, Wis.) added at a 1:50 (w/w) enzyme to protein ratio. Digestions were quenched by the addition of trifluoroacetic acid (TFA, Thermo Pierce) and were desalted over iC18 Sep-Pak cartridges (Waters, Milford, Mass.).

For online nanoflow liquid chromatography tandem mass spectrometry (nLC-MS/MS), reversed phase columns were packed-in house using 75 µm ID, 360 µm OD bare fused silica capillary. A nanoelectrospray tip was laser pulled (Sutter Instrument Company, Novato, Calif.) and packed with 1.7 µm diameter, 130 Å pore size Ethylene Bridged Hybrid C18 particles (Waters) to a length of 30-35 cm. Buffer A consisted of 0.2% formic acid and 5% DMSO in water, and Buffer B consisted of 0.2% formic acid in acetonitrile. Two µg of peptides were loaded onto the column in 95% buffer A for 12 min at 300 min-1. Gradient elution was performed at 300 nL min-1 and gradients increased linearly from 5 to 35% buffer B over 190 minutes, followed by an increase to 70% B at 215 minutes and a wash at 70% B for 5 minutes. The column was then re-equilibrated at 5% B for 20 minutes. Eluting peptide were ionized with electrospray ionization at +2 kV, and the inlet capillary temperature was held at 300° C. on an ion trap-Orbitrap hybrid mass spectrometer (Orbitrap Elite, Thermo Fisher Scientific, San Jose, Calif.). Survey scans of peptide precursors were collected over the 300-1500 Thompson range in the Orbitrap with an automatic gain control target value of 1,000,000 (50 ms maximum injection time), followed by data-dependent ion trap MS/MS scans using collisional activation dissociation (CAD) of the 20 most intense peaks (AGC target value of 5,000 and maximum injection times of 100 ms). Precursors with charge states equal to one or unassigned were rejected.

Raw data was processed using MaxQuant version 1.4.1.268, and tandem mass spectra were searched with the Andromeda search algorithm. Oxidation of methionine was specified as a variable modification, while carbamidomethylation of cysteine was a set as a fixed modification. A precursor search tolerance of 20 ppm and a product mass tolerance of 0.35 Da were used for searches, and three missed cleavages were allowed for full trypsin specificity. Peptide spectral matches (PSMs) were made against a target-decoy custom database of the yeast strain was used, which was concatenated with a reversed sequence version of the forward database from McIlwain et al. Peptides were filtered to a 1% false discovery rate (FDR) and a 1% protein FDR was applied according to the target-decoy method. Proteins were identified using at least one peptide (razor+unique), where razor peptide is defined as a non-unique peptide assigned to the protein group with the most other peptides (Occam's razor principle). Proteins were quantified and normalized using MaxLFQ with a label-free quantification (LFQ) minimum ratio count of 2. LFQ intensities were calculated using the match between runs feature, and MS/MS spectra were not required for LFQ comparisons. For quantitative comparisons, protein intensity values were log 2 transformed prior to further analysis. All possible proteins were analyzed as long as the proteins were identified in both strains being compared, to maximize data obtained from this analysis. In total, 3,550 unique proteins were identified in across all strains and conditions. All raw mass spectrometry files and associated information about identifications are available on Chorus under Project ID 999 and Experiment ID 3007.

Correlation between transcriptomic and proteomic differences across media conditions. The response to anaerobiosis was calculated for each strain growing either on glucose or xylose, as the log 2 of mRNA or protein abundance in glucose-O₂/glucose+O₂ or xylose-O₂/xylose+O₂. The replicate-averaged log 2(fold-change) in mRNA was compared to the log 2(fold-change) in protein for each strain (FIG. 1A).

Phosphoproteomic analysis. Phosphoproteomic experiments were multiplexed using tandem mass tags (TMT) isobaric labels to quantitatively compare the phosphoproteomes of Y22-3, Y127, and Y128 yeast strains. 6-plex experiments were performed to compare the three strains grown on xylose under aerobic and anaerobic conditions. Yeast phosphoproteomes were obtained from cell pellets from the same cultures used for the label free experiments described above using the same protein extraction, proteolytic digestion, and desalting conditions. A second phosphoproteomic experiment used TMT tags to compare the phosphoproteomic profiles of Y184, Y184 ira2Δ, and Y184 bcy1Δ during anaerobic growth on xylose in duplicate, using the same collection and methods outlined above.

Following the generation of tryptic peptides, 500 µg of peptides from each condition were labeled with TMT 6-plex isobaric labels (Thermo Pierce) by re-suspending peptides in 200 µL of freshly made 200 mM triethylammonium bicarbonate (TEAB) and combining with 50 µL of the TMT labeling reagent resuspended in 100% acetonitrile. The samples were labeled for 4 hours, then ~5 µg of material from each TMT channel was combined into a test mix and analyzed by LC-MS/MS to evaluate labeling efficiency and obtain optimal ratios for sample recombination. Samples were quenched with 1.6 µL of 50% hydroxylamine, then combined in equal amounts by mass, and desalted.

Combined TMT-labeled peptides were then enriched for phospho-peptides using immobilized metal affinity chroma-

tography (IMAC) with magnetic beads (Qiagen, Valencia, Calif.). After equilibration with water, the magnetic beads were incubated with 40 mM EDTA (pH 8.0) for 30 minutes while shaking. This process was repeated for a total of two incubations. Next, the beads were washed four times with water and incubated with 30 mM FeCl₃ for 30 minutes while shaking, and this was also repeated for a total of two incubations. Beads were then washed four times with 80% acetonitrile/0.15% TFA. The TMT-labeled peptides were re-suspended in 80% acetonitrile/0.15% TFA and incubated with the magnetic beads for 45 minutes with shaking. Unbound peptides were collected for protein analysis. Bound peptides were washed three times with 80% acetonitrile/0.15% TFA and eluted with 50% acetonitrile, 0.7% NH₄OH. Eluted peptides were immediately acidified with 4% formic acid, frozen, and lyophilized. Enriched phosphopeptides were re-suspended in 20 μ L 0.2% FA for LC-MS/MS analysis.

Online nanoflow liquid chromatography tandem mass spectrometry (nLC-MS/MS) was performed similarly as to the methods described above, including the same LC system and buffers, capillary reversed phase columns, gradient, and MS system and electrospray conditions. TMT phosphoproteomic experiments were also performed as single-shot (i.e., no fractionation) four-hour experiments. Survey scans of peptide precursors were collected over the 300-1500 Thompson range in the Orbitrap with a resolving power of 60,000 at 400 m/z and an automatic gain control target value of 1,000,000 (75 ms maximum injection time), followed by data-dependent MS/MS scans in the Orbitrap (resolving power 15,000 at 400 m/z) using higher-energy collisional dissociation (HCD, normalized collision energy of 35) of the 15 most intense peaks (AGC target value of 50,000 and maximum injection times of 200 ms). The first mass of MS/MS scans was fixed at 120 m/z, precursors were isolated with 1.8 Th isolation width, and precursors with charge states equal to one or unassigned were rejected. Dynamic exclusion windows were created around monoisotopic precursor peaks using 10 ppm windows, and the exclusion duration lasted for 40 seconds. Two technical replicate injections of each sample were performed.

Data processing for the TMT phosphoproteomic experiments used COMPASS. The Open Mass Spectrometry Search Algorithm (OMSSA) searches were performed against the same target-decoy yeast database used in the label free experiments described above. Searches were conducted using a 125 ppm precursor mass tolerance and a 0.02 Da product mass tolerance. A maximum of 3 missed tryptic cleavages were allowed. Fixed modifications were carbamidomethylation of cysteine residues, TMT 6-plex label on peptide N-termini, and TMT 6-plex on lysine. Variable modifications included oxidation of methionine; TMT 6-plex on tyrosine residues; phosphorylation of serine, threonine, and tyrosine residues; and neutral loss of phosphorylation on serine and threonine residues. A false discovery rate of 1% was used at the peptide and protein level. Within COMPASS, TMT quantification was performed and quantified peptides were grouped into proteins as described. Phospho-peptide localization was performed using phosphoRS73 integrated with COMPASS, using 75% as a localization probability cutoff to determine localized phosphosites. Phospho-peptides with non-localized phospho-sites were discarded from further analysis. TMT reporter ion intensities were normalized for changes in protein level and log₂ transformed prior to further analysis. The Phospho-GRID database was used to identify phospho-sites of known function. All raw mass spectrometry files and associated

information about identifications are available on Chorus under Project ID 999 and Experiment IDs 3016 and 3166.

Phosphoproteomic network analysis. The inventors developed a novel network approach to infer kinases and phosphatases that mediate phosphoproteomic changes across the strain panel. The method predicts co-regulated groups of phospho-peptides, called modules, and then searches a background network of protein-protein interactions to identify 'shared interactor' proteins that physically interact with more module constituent proteins than expected by chance. The method consists of four steps: to identify potentially co-regulated peptides, the method 1) classifies phosphopeptides according to phosphorylation profiles across strains and then 2) within each class, partitions peptides into 'modules' of peptides that share the same motif around the phosphorylated site ('phospho-motif'). 3) To identify potential regulators of each module, the method identifies 'shared interactor' proteins that physically interact with more module constituents than expected by chance, and then 4) identifies the subset of shared interactors that are kinases and phosphatases, focusing on regulators whose known specificity matches the target module phospho-motif. These steps are described in more detail below.

1) Classifying Phospho-peptides. Phospho-peptides were partitioned into four classes based on the log₂(fold-change) in phosphorylation in each strain grown in xylose-O₂ versus xylose+O₂. Class A contained phospho-peptides that show progressive increases or decreases in phosphorylation response (at least 1.5 fold difference in replicate-averaged log₂ expression changes, as described above) across Y22-3, Y127, and Y128. This identified 182 phospho-peptides from 154 proteins that showed a progressive increase in response across Y22-3, Y127, and Y128 and 225 phospho-peptides from 150 proteins that showed a progressive decrease in response across the strains; these were separated into "Class A-increasing" and "Class A-decreasing" groups. Class B contained phospho-peptides with a unique hypoxic response in xylose in Y128 (at least 1.5 fold absolute difference in Y128 compared to both Y127 and Y22-3, and no significant difference between Y127 and Y22-3). This identified 108 phospho-peptides from 96 proteins that showed a larger response in Y128 and 157 phospho-peptides from 138 proteins that showed a smaller log₂ fold-change in Y128; these were separated into "Class B-increasing" and "Class B-decreasing" groups.

2) Identifying phosphorylation motifs. Peptides from each of the four classes defined above were partitioned into modules using the program motif-X using the following parameters: extend from SGD yeast proteome; central character as s* or t*; motif width of 13; motif occurrences of 10; motif significance 1 \times 10⁻⁶. Three total motifs were identified for Class A and five total motifs were identified for Class B. Groups of phospho-peptides containing the same motif are referred to as modules.

3) Identifying Shared Interactor proteins. Under the assumption that co-regulated peptides interact with the same responsible regulator, the inventors searched a background dataset of protein-protein interactions to identify 'shared interactors' (SIs) that interact with more module constituents than expected by chance, using a custom Python script. The background network was taken from a previously compiled collection of high and low-throughput protein-protein interactions or kinase-substrate interactions in *S. cerevisiae* and contains 4,638 proteins and 25,682 directed and non-directed interactions. For each module, the script identifies all proteins from the background network that interact with more module constituent proteins than expected by chance

(hypergeometric test), using Benjamini-Hochberg correction and an $FDR < 0.05$ as significant. This analysis revealed 59 SIs connected to Class A modules and 90 SIs connected to Class B modules.

4) Identifying candidate module regulators. The inventors focused on the subset of SIs that are kinases with known specificity and phosphatases whose interactions with the module were primarily directed toward module constituents or were undirected. For the kinases with known specificity, the inventors scored if the module phosphorylation motif matched the kinase motif as follows: Briefly, a position-weight matrix (PWM) was constructed for each module and compared to the PWM representing known kinase phosphorylation preferences from Mok et al. These PWMs were generated from a peptide phosphorylation spot array assay where the normalized, background-corrected value is provided as a weight for each amino acid at each position, which was converted to a frequency value by calculating the total of all signal intensities for all amino acids at each position and then dividing by the total sum of the intensities. A pseudocount was used to prevent overfitting and to remove zeros that may occur in the Mok et al. PWMs. These generated kinase PWMs were compared to the motif-X motifs via Kullback-Leibler Divergence (KLD). Statistical significance of matches was determined using a distribution of KLD scores generated from randomizing the within-column values and then shuffling the columns themselves 1000 times. This generated 63,000 random KLD scores per module motif. FDR was calculated as the number of random KLD scores with smaller values than the observed value. Kinases whose known specificity matched the module phosphorylation motif were retained for further consideration along with identified phosphatases. Using this approach, 6 kinases and 2 phosphatases were identified for Class A modules and 5 kinases were identified for Class B modules. Networks were visualized using Cytoscape (version 3.4.0).

Phosphoproteomic analysis across strains with and without BCY1. The inventors identified phospho-peptides with a reproducible log 2 expression difference of at least 1.5 \times in both biological replicates in Y184 *bcy1* Δ compared to Y184 (which mimics Y127) or in Y184 *bcy1* Δ compared to Y184 *ira2* Δ (which mimics Y128). Phospho-peptides were clustered using MClust version 4.457 and visualized using Java TreeView (<http://jtreeview.sourceforge.net>). Functional enrichment analysis was performed with a hypergeometric test using data sets compiled of up-to-date GO annotation terms (downloaded 2017-10-18), using as the background dataset the starting set of peptides used in this analysis. Phosphorylation motifs were identified as described above using motif-X.

Metabolomics analysis. Metabolite data from Sato et al. was analyzed to compare changes in Y128 xylose- O_2 versus Y22-3 xylose- O_2 . A paired T-test was used to compare changes and those with a p -value ≤ 0.05 were considered significant.

Inhibition of growth using hydroxyurea. Growth inhibition was performed using 400 mM hydroxyurea, added after 17 hours of anaerobic growth in xylose. Before and after growth inhibition, OD_{600} as well as sugar and ethanol concentrations were measured as above.

PKA activity assay. Measurement of PKA activity was performed on lysed cells using the PKA Kinase Activity Assay Kit from ABCAM. Cultures were grown anaerobically in xylose for three doublings (to $OD_{600} \sim 0.5$), at which 10 mL of cells were collected by centrifugation for 3 minutes at 3000 rpm, in preparation for lysis. Supernatant was removed under anaerobic conditions and the cells were

resuspended in 1 mL of SB buffer (1 M sorbitol, 20 mM Tris HCl, pH 7.4) with 300 units of zymolyase (Amsbio) and 10 μ L of protease inhibitor cocktail IV (Millipore). Cells were incubated for 10 minutes at 30 $^\circ$ C. anaerobically. Cells were collected by centrifugation for 5 minutes at 350 \times g and washed 1 \times with SB buffer under anaerobic conditions. Cells were resuspended in 750 μ L HLB buffer (10 mM Tris HCl, pH 7.4, 10 mM NaCl, 3 mM $MgCl_2$, 0.3% (vol/vol) NP-40, 10% (vol/vol) glycerol) with 10 μ L protease inhibitor cocktail IV and incubated on ice for 10 minutes, anaerobically. Cultures were subjected to ten rounds in a Dounce homogenizer anaerobically to promote lysis. Lysis was verified using microscopy and total protein abundance was determined using a Bradford assay. 200 μ L of cell lysate was removed and 50 μ M H-89 was added as a PKA inhibitor and incubated for 10 minutes at 30 $^\circ$ C. anaerobically. The PKA Kinase Activity Assay Kit was performed following manufacture's protocol, with the kinase reaction occurring under anaerobic conditions and the remaining steps (primary and secondary antibody incubation and washes) being performed aerobically. The reaction was detected using a TECAN Infinite 200 Pro with a wavelength of 450 nm. Positive (active PKA provided by ABCAM) and negative (no cells, blank) controls were used for each experimental reaction as verification of kit functionality. Relative PKA activity was calculated by subtracting the measured absorbance for each sample from the absorbance from the blank to remove background, followed by normalization to total protein abundance for each sample. Paired T-tests were used to determine significant differences among samples.

Sugar consumption rate calculations. Sugar consumption rates were calculated with a rate estimation tool as described previously using cell density (OD_{600}) and extracellular sugar concentrations measured by HPLC-RID. Log 2 data from each of three independent biological replicates were fit with linear models, and xylose consumption rate was calculated as g/L/ OD_{600} /hour. Rates calculated for each replicate were plotted and compared with a paired T-test.

BCY1-AiD fermentations. Experiments were designed to mimic high-cell titer industrial fermentations. Cells were grown in YP-6% glucose or YP-3% xylose to match sugar concentrations in hydrolysate. Strain Y184 Bcy1-AiD was grown aerobically in 6% glucose medium starting at an OD_{600} 0.1 or grown anaerobically in 3% xylose medium starting at OD_{600} 4.0. The tagged strain was compared to Y128, Y184 and Y184 *bcy1* Δ . OD_{600} and glucose, xylose, and ethanol were measured and rates were determined as described above. Bcy1-AiD stability was measured for each experiment using Western blot analysis as described previously. Because the AiD tag contained a 3 \times -FLAG sequence, α -FLAG antibody (1:2500, Sigma) was used to detect Bcy1-AiD while α -Actin antibody (1:2500, Pierce) was used to detect actin as a loading control. The blot in FIG. 16 is representative of biological triplicates.

Example 3

Phosphoproteomics in Y184 BCY1 Δ Implicates Responses Involved in Ggrowth Versus Metabolism

The inventors compared phosphoproteomic data among three strains cultured anaerobically on xylose: Y184 (Y22-3 *gre3* Δ *isu1* Δ) that can neither grow on nor metabolize xylose, Y184 *ira2* Δ (Y22-3 *gre3* Δ *isu1* Δ *ira2* Δ) that both grows on and metabolizes xylose, and Y184 *bcy1* Δ (Y22-3 *gre3* Δ *isu1* Δ *bcy1* Δ) that does not grow on but metabolizes xylose. In total, 541 phospho-peptides showed a ≥ 1.5 fold

difference in abundance between Y184 *bcy1Δ* and Y184 or Y184 *ira2Δ*, in both biological replicates. These peptides were classified into three groups: Class I peptides are those with a difference in phosphorylation level in Y184 *bcy1Δ* cultured anaerobically on xylose relative to both Y184 and Y184 *ira2Δ* cultured under those conditions. Class II peptides are those with differences between the Y184 *bcy1Δ* strain compared to Y184 *ira2Δ* only—Class II peptides therefore represent those where the *bcy1Δ* strain was more similar to Y184, neither of which grows anaerobically on xylose. Class III peptides are those whose phosphorylation was reproducibly different only in the *bcy1Δ* strain compared to Y184, revealing that the *bcy1Δ* strain behaved more like the Y184 *ira2Δ* strain, which can also metabolize xylose (FIG. 4B-4D). The inventors examined each cluster using enrichment and network analysis, under the hypotheses that Class II phospho-peptides may relate to the growth defect of Y127 and Y184 *bcy1Δ* whereas Class III phospho-peptides may be those associated with xylose metabolism, since both Y128 and Y184 *bcy1Δ* can metabolize the sugar under these conditions.

There were 188 phosphorylation events in Class I, unique to or amplified in the *bcy1Δ* strain compared to both Y184 and Y184 *ira2Δ*. These included 34 phospho-peptides (in 28 proteins) that showed increased phosphorylation in *bcy1Δ* and 154 phospho-peptides (mapping to 111 proteins) with a *bcy1Δ*-specific decrease (FIG. 4B). Both groups included proteins related to the stress response and glycolysis. Interestingly, the *bcy1Δ* strain cultured anaerobically on xylose showed increased phosphorylation of serine 248 (S248) of Pbs2, the MAPKKK that activates the Hog1 kinase; in contrast, the strain showed reduced phosphorylation of T174 on Hog1, whose phosphorylation normally activates the kinase. This is especially intriguing because Hog1 inactivation in Y127 and other strains enhances xylose consumption. The inventors' data suggest that BCY1 deletion serves to down-regulate Hog1 signaling without mutation of the gene. The inventors previously proposed that Hog1 activity during glucose starvation may reduce growth-promoting processes, and thus deleting HOG1 (or down-regulating its activity) may enable xylose fermentation without the corresponding limitation of growth related processes.

Multiple hexokinases were affected uniquely in the *bcy1Δ* strain: Glk1 and Hxk1 both showed increased phosphorylation in the strain, whereas the main hexokinase, HXK2, showed decreased phosphorylation on many sites (several shared with Y184 *ira2Δ*). These included reduced phosphorylation on S158 that is normally autophosphorylated as a feedback mechanism to inactivate the enzyme, and S1536 whose phosphorylation normally increases activity, see below. HXK2 is an interesting enzyme, because it acts both in glycolysis and as a regulator of nuclear transcription via the Mig1 repressor. Decreased phosphorylation at these sites may have broader effects here: deletion of HXK2 results in constitutive expression of Snf1 targets to enable growth on non-glucose fermentable carbon sources. The inventors' data raise the possibility that hexokinase activity is decreased to affect how the cell senses and/or responds to glucose availability.

The inventors next analyzed phosphoproteomic changes in Class II, where the *bcy1Δ* strain (which metabolizes xylose but cannot grow on it) is more similar to Y184 that can neither grow nor metabolize xylose (FIG. 4C). The inventors' hypothesis is that phosphorylation of peptides in this category may be related to the shared inability of these strains to grow anaerobically on xylose. There were 22 phospho-sites (in 18 proteins) with an increase in phospho-

rylation in Y184 *bcy1Δ* compared to Y184 *ira2Δ*. Although there was no significant enrichment, there were several interesting proteins including transketolase (Tkl1) involved in pentose phosphate/xylose metabolism and intriguingly Rnr2, the main deoxyribonucleotide-diphosphate reductase critical for nucleotide biosynthesis and thus growth. Conversely, 28 phospho-sites (in 24 proteins) showed decreased phosphorylation in the *bcy1Δ* strain compared to Y184 *ira2Δ*. These included several proteins involved in ribosome biogenesis (Alb1 and Zuo1), mRNA transport (Nup60), as well as Mga2 discussed in the main text. It is possible that one or more of these phosphorylation differences inhibit growth in the *bcy1Δ* strain but enable continued xylose fermentation.

In contrast, Class III phosphorylation events were similar between Y184 *bcy1Δ* and Y184 *ira2Δ* strains, but distinct from Y184 that cannot metabolize xylose (FIG. 4D). The 51 phospho-sites (in 38 proteins) that displayed an increase in phosphorylation in the *bcy1Δ* strain compared to Y184 were enriched for stress response proteins, including the Yak1 kinase that is antagonistic to PKA signaling and activated during times of stress^{3,4}. Since PKA activity is known to suppress the stress response, this signature likely reflects PKA-dependent suppression of stress defense. Also included in the group of peptides with higher phosphorylation in xylose-fermenting strains is Cdc25, the guanine-nucleotide exchange factor for RAS and a known PKA target. Increased phosphorylation on Cdc25 site S135 is thought to increase its activity, which would promote RAS-dependent signaling and PKA activity⁸⁹. The increased phosphorylation of Cdc25 S135 is consistent with the notion that RAS/PKA activity is up-regulated by IRA2 or BCY1 deletion to promote increased xylose flux. The 262 phospho-sites (in 165 proteins) that showed a decrease in phosphorylation compared to Y184 were enriched for proteins involved in the regulation of cell shape, cytoskeleton, and bud site selection. Interestingly, network analysis revealed that Pkh1 (involved in endocytosis control), Yck2 (involved in morphogenesis, trafficking, and glucose response), Akl1 (endocytosis and cytoskeleton organization), and Ark1 (regulation of actin cytoskeleton) kinases all showed more interactions with the proteins whose phosphorylation decreased in this class, compared to what is expected by chance. Indeed, many of the 165 proteins to which the affected peptides mapped are involved in cytoskeleton regulation. Several other sites with decreased phosphorylation in the *bcy1Δ* and Y184 *ira2Δ* strains have known functions related to cell cycle progression, including histone Hta1 on S129 and Cdc3 on site S50390. Decreased phosphorylation of Pahl1 and Cho1 involved in lipid biogenesis is also predicted to reduce activity of the enzymes. It is intriguing that so many of these regulators are linked to growth, morphology, and cell-cycle progression; however, their phosphorylation patterns are shared between the growing Y184 *ira2Δ* and the arrested Y184 *bcy1Δ*. One possibility is that these phosphorylation events are a unique response in the Y184 reference strain in response to its inability to grow, for reasons that are distinct than in Y184 *bcy1Δ*.

As can be appreciated, the results described in the above examples support the utility of the nucleic acids, yeast strains and methods described and claimed herein for enhancing biofuel production in yeast. Other embodiments and uses of the invention will be apparent to those skilled in the art from consideration from the specification and practice of the invention disclosed herein. All references cited herein for any reason, including all journal citations and U.S./foreign patents and patent applications, are specifically

and entirely incorporated herein by reference. It is understood that the invention is not confined to the specific materials, methods, formulations, reaction/assay conditions, etc., herein illustrated and described, but embraces such modified forms thereof as come within the scope of the following claims.

REFERENCES:

1. Kricka, W., Fitzpatrick, J. & Bond, U. Challenges for the production of bioethanol from biomass using recombinant yeasts. *Adv Appl Microbiol* 92, 89-125 (2015).
2. Moysés, D. N., Reis, V. C. B., de Almeida, J. R. M., de Moraes, L. M. P. & Torres, F. A. G. Xylose Fermentation by *Saccharomyces cerevisiae*: Challenges and Prospects. *Int J Mol Sci* 17, 207 (2016).
3. Smets, B. et al. Life in the midst of scarcity: adaptations to nutrient availability in *Saccharomyces cerevisiae*. *Curr Genet* 56, 1-32 (2010).
4. Conrad, M. et al. Nutrient sensing and signaling in the yeast *Saccharomyces cerevisiae*. *FEMS Microbiol Rev* 38, 254-299 (2014).
5. Kayikci, Ö. & Nielsen, J. Glucose repression in *Saccharomyces cerevisiae*. *FEMS Yeast Res* 15, fov068 (2015).
6. Parreiras, L. S. et al. Engineering and Two-Stage Evolution of a Lignocellulosic Hydrolysate-Tolerant *Saccharomyces cerevisiae* Strain for Anaerobic Fermentation of Xylose from AFEX Pretreated Corn Stover. *PLoS ONE* 9, e107499 (2014).
7. Sato, T. K. et al. Directed Evolution Reveals Unexpected Epistatic Interactions That Alter Metabolic Regulation and Enable Anaerobic Xylose Use by *Saccharomyces cerevisiae*. *PLoS Genetics* 12, e1006372 (2016).
8. Matsushika, A., Goshima, T. & Hoshino, T. Transcription analysis of recombinant industrial and laboratory *Saccharomyces cerevisiae* strains reveals the molecular basis for fermentation of glucose and xylose. *Microb Cell Fact* 13, 16 (2014).
9. Li, Y.-C. et al. Transcriptome changes in adaptive evolution of xylose-fermenting industrial *Saccharomyces cerevisiae* strains with 8-integration of different xylA genes. *Appl. Microbiol. Biotechnol.* 101, 7741-7753 (2017).
10. Schwelberger, H. G., Kang, H. A. & Hershey, J. W. Translation initiation factor eIF-5A expressed from either of two yeast genes or from human cDNA. Functional identity under aerobic and anaerobic conditions. *J Biol Chem* 268, 14018-14025 (1993).
11. Stein, T., Kricke, J., Becher, D. & Lisowsky, T. Azf1p is a nuclear-localized zinc-finger protein that is preferentially expressed under non-fermentative growth conditions in *Saccharomyces cerevisiae*. *Curr Genet* 34, 287-296 (1998).
12. Newcomb, L. L., Hall, D. D. & Heideman, W. AZF 1 is a glucose-dependent positive regulator of CLN3 transcription in *Saccharomyces cerevisiae*. *Mol Cell Biol* 22, 1607-1614 (2002).
13. Slattery, M. G., Liko, D. & Heideman, W. The function and properties of the Azf1 transcriptional regulator change with growth conditions in *Saccharomyces cerevisiae*. *Eukaryot Cell* 5, 313-320 (2006).
14. Bolotin-Fukuhara, M. Thirty years of the HAP2/3/4/5 complex. *Biochimica et Biophysica Acta (BBA)-Gene Regulatory Mechanisms* 1860, 543-559 (2017).
15. Martinez-Pastor, M. T. et al. The *Saccharomyces cerevisiae* zinc finger proteins Msn2p and Msn4p are required for transcriptional induction through the stress response element (STRE). *EMBO J* 15, 2227-2235 (1996).
16. Michael, D. G. et al. Model-based transcriptome engineering promotes a fermentative transcriptional state in yeast. *Proc Natl Acad Sci USA* 113, E7428-E7437 (2016).
17. Roy, A., Jouandot, D., Cho, K. H. & Kim, J.-H. Understanding the mechanism of glucose-induced relief of Rgt1-mediated repression in yeast. *FEBS Open Bio* 4, 105-111 (2014).
18. Jiang, Y. et al. MGA2 is involved in the low-oxygen response element-dependent hypoxic induction of genes in *Saccharomyces cerevisiae*. *Mol Cell Biol* 21, 6161-6169 (2001).
19. MacGilvray, M. E. et al. Network inference reveals novel connections in pathways regulating growth and defense in the yeast salt response. *PLoS Comput Biol* 13, e1006088 (2018).
20. Homma, M. K. et al. CK2 phosphorylation of eukaryotic translation initiation factor 5 potentiates cell cycle progression. *Proc Natl Acad Sci USA* 102, 15688-15693 (2005).
21. Kallmeyer, A. K., Keeling, K. M. & Bedwell, D. M. Eukaryotic release factor 1 phosphorylation by CK2 protein kinase is dynamic but has little effect on the efficiency of translation termination in *Saccharomyces cerevisiae*. *Eukaryot Cell* 5, 1378-1387 (2006).
22. Gandin, V. et al. mTORC1 and CK2 coordinate ternary and eIF4F complex assembly. *Nat Comms* 7, 11127 (2016).
23. Ewald, J. C., Kuehne, A., Zamboni, N. & Skotheim, J. M. The Yeast Cyclin-Dependent Kinase Routes Carbon Fluxes to Fuel Cell Cycle Progression. *Mol Cell* 62, 532-545 (2016).
24. Zhao, G., Chen, Y., Carey, L. & Futcher, B. Cyclin-Dependent Kinase Co-Ordinates Carbohydrate Metabolism and Cell Cycle in *S. cerevisiae*. *Mol Cell* 62, 546-557 (2016).
25. Broach, J. R. Nutritional Control of Growth and Development in Yeast. *Genetics* 192, 73-105 (2012).
26. Colombo, S., Ronchetti, D., Thevelein, J. M., Winderickx, J. & Martegani, E. Activation state of the Ras2 protein and glucose-induced signaling in *Saccharomyces cerevisiae*. *J Biol Chem* 279, 46715-46722 (2004).
27. Garreau, H. et al. Hyperphosphorylation of Msn2p and Msn4p in response to heat shock and the diauxic shift is inhibited by cAMP in *Saccharomyces cerevisiae*. *Microbiology* 146, 2113-2120 (2000).
28. Costanzo, M. et al. The genetic landscape of a cell. *Science* 327, 425-431 (2010).
29. Zaman, S., Lippman, S. I., Schnepfer, L., Slonim, N. & Broach, J. R. Glucose regulates transcription in yeast through a network of signaling pathways. *Mol Syst Biol* 5, 245 (2009).
30. Mosch, H.-U., Kubler, E., Krappmann, S., Fink, G. R. & Braus, G. H. Crosstalk between the Ras2p-controlled Mitogen-activated Protein Kinase and cAMP Pathways during Invasive Growth of *Saccharomyces cerevisiae*. *MBC* 10, 1325-1335 (1999).
31. Ho, J. & Bretscher, A. Ras regulates the polarity of the yeast actin cytoskeleton through the stress response pathway. *Molecular Biology of the Cell* 12, 1541-1555 (2001).
32. Weeks, G. & Spiegelman, G. B. Roles played by Ras subfamily proteins in the cell and developmental biology of microorganisms. *Cell Signal* 15, 901-909 (2003).
33. Cannon, J. F. & Tatchell, K. Characterization of *Saccharomyces cerevisiae* genes encoding subunits of cyclic AMP-dependent protein kinase. *Mol Cell Biol* 7, 2653-2663 (1987).

34. Cai, Z., Zhang, B. & Li, Y. Engineering *Saccharomyces cerevisiae* for efficient anaerobic xylose fermentation: reflections and perspectives. *Biotechnol J* 7, 34-46 (2012).
35. Vilela, L. de F. et al. Enhanced xylose fermentation and ethanol production by engineered *Saccharomyces cerevisiae* strain. *AMB Express* 5, 16 (2015).
36. Kriegel, T. M., Rush, J., Vojtek, A. B., Clifton, D. & Fraenkel, D. G. In vivo phosphorylation site of hexokinase 2 in *Saccharomyces cerevisiae*. *Biochemistry* 33, 148-152 (1994).
37. Warmka, J., Hanneman, J., Lee, J., Amin, D. & Ota, I. Ptc1, a type 2C Ser/Thr phosphatase, inactivates the HOG pathway by dephosphorylating the mitogen-activated protein kinase Hog1. *Mol Cell Biol* 21, 51-60 (2001).
38. Santos, dos, L. V. et al. Unraveling the genetic basis of xylose consumption in engineered *Saccharomyces cerevisiae* strains. *Sci Rep* 6, 38676 (2016).
39. Nishimura, K., Fukagawa, T., Takisawa, H., Kakimoto, T. & Kanemaki, M. An auxin-based degron system for the rapid depletion of proteins in nonplant cells. *Nat Methods* 6, 917-922 (2009).
40. Van de Velde, S. & Thevelein, J. M. Cyclic AMP-protein kinase A and Snf1 signaling mechanisms underlie the superior potency of sucrose for induction of filamentation in *Saccharomyces cerevisiae*. *Eukaryot Cell* 7, 286-293 (2008).
41. Shively, C. A. et al. Large-Scale Analysis of Kinase Signaling in Yeast Pseudohyphal Development Identifies Regulation of Ribonucleoprotein Granules. *PLoS Genetics* 11, e1005564 (2015).
42. Griffioen, G. & Thevelein, J. M. Molecular mechanisms controlling the localisation of protein kinase A. *Curr Genet* 41, 199-207 (2002).
43. Galello, F., Moreno, S. & Rossi, S. Interacting proteins of protein kinase A regulatory subunit in *Saccharomyces cerevisiae*. *Journal of Proteomics* 109, 261-275 (2014).
44. Smith, F. D. et al. Local protein kinase A action proceeds through intact holoenzymes. *Science* 356, 1288-1293 (2017).
45. Mok, J. et al. Deciphering Protein Kinase Specificity through Large-Scale Analysis of Yeast Phosphorylation Site Motifs. *Sci. Signal.* 3, ra12-ra12 (2010).
46. Magtanong, L. et al. Dosage suppression genetic interaction networks enhance functional wiring diagrams of the cell. *Nat Biotechnol* 29, 505-511 (2011).
47. Morawska, M. & Ulrich, H. D. An expanded tool kit for the auxin-inducible degron system in budding yeast. *Yeast* 30, 341-351 (2013).
48. Tanaka, S., Miyazawa Onami, M., Iida, T. & Araki, H. iAID: an improved auxin-inducible degron system for the construction of a 'tight' conditional mutant in the budding yeast *Saccharomyces cerevisiae*. *Yeast* 32, 567-581 (2015).
49. Nishimura, K. & Kanemaki, M. T. Rapid Depletion of Budding Yeast Proteins via the Fusion of an Auxin-Inducible Degron (AID). *Curr Protoc Cell Biol* 64, 20.9.1-16 (2014).
50. Gasch, A. P. in *Guide to Yeast Genetics and Molecular and Cell Biology—Part B* 350, 393-414 (Elsevier, 2002).
51. Bolger, A. M., Lohse, M. & Usadel, B. Trimmomatic: a flexible trimmer for Illumina sequence data. *Bioinformatics* 30, 2114-2120 (2014).
52. McIlwain, S. J. et al. Genome sequence and analysis of a stress-tolerant, wild-derived strain of *Saccharomyces cerevisiae* used in biofuels research. G36, 1757-1766 (2016).

53. Langmead, B. Aligning short sequencing reads with Bowtie. *Curr Protoc Bioinformatics* 17, (2010).
54. Anders, S., Pyl, P. T. & Huber, W. HTSeq—A Python framework to work with high-throughput sequencing data. *Bioinformatics* 31, btu638-169 (2014).
55. Robinson, M., McCarthy, D. & Smyth, G. edgeR: a Bioconductor package for differential expression analysis of digital gene expression data. *Bioinformatics* 26, 139 (2010).
56. Benjamini, Y. & Hochberg, Y. Controlling the false discovery rate: a practical and powerful approach to multiple testing. *Journal of the Royal Statistical Society Series B (Methodological)* 57, 289-300 (1995).
57. Fraley, C. & Raftery, A. E. Model-Based Clustering, Discriminant Analysis, and Density Estimation. *J Am Stat Assoc* 97, 611-631 (2011).
58. Saldanha, A. J. Java Treeview—extensible visualization of microarray data. *Bioinformatics* 20, 3246-3248 (2004).
59. Robinson, M. D., Grigull, J., Mohammad, N. & Hughes, T. R. FunSpec: a web-based cluster interpreter for yeast. *BMC Bioinformatics* 3, 35 (2002).
60. Boyle, E. I. et al. GO::TermFinder—open source software for accessing Gene Ontology information and finding significantly enriched Gene Ontology terms associated with a list of genes. *Bioinformatics* 20, 3710-3715 (2004).
61. Chasman, D. et al. Pathway connectivity and signaling coordination in the yeast stress-activated signaling network. *Mol Syst Biol* 10, 759-759 (2014).
62. Teixeira, M. C. et al. The YEASTRACT database: an upgraded information system for the analysis of gene and genomic transcription regulation in *Saccharomyces cerevisiae*. 42, D161-D166 (2014).
63. Bailey, T. L., Williams, N., Misleh, C. & Li, W. W. MEME: discovering and analyzing DNA and protein sequence motifs. 34, W369-73 (2006).
64. Gupta, S., Stamatoyannopoulos, J. A., Bailey, T. L. & Noble, W. Quantifying similarity between motifs. *Genome Biol* 8, R24 (2007).
65. Crooks, G. E., Hon, G., Chandonia, J.-M. & Brenner, S. E. WebLogo: a sequence logo generator. *Genome Res* 14, 1188-1190 (2004).
66. Bailey, T. L. & Gribskov, M. Combining evidence using p-values: application to sequence homology searches. *Bioinformatics* 14, 48-54 (1998).
67. Hebert, A. S. et al. The one hour yeast proteome. *Mol. Cell Proteomics* 13, 339-347 (2014).
68. Cox, J. & Mann, M. MaxQuant enables high peptide identification rates, individualized p.p.b.-range mass accuracies and proteome-wide protein quantification. *Nat Biotechnol* 26, 1367-1372 (2008).
69. Cox, J. et al. Andromeda: a peptide search engine integrated into the MaxQuant environment. *J Proteome Res.* 10, 1794-1805 (2011).
70. Cox, J. et al. Accurate Proteome-wide Label-free Quantification by Delayed Normalization and Maximal Peptide Ratio Extraction, Termed MaxLFQ. *Mol. Cell Proteomics* 13, 2513-2526 (2014).
71. Wenger, C. D., Phanstiel, D. H., Lee, M. V., Bailey, D. J. & Coon, J. J. COMPASS: A suite of pre- and post-search proteomics software tools for OMSSA. *Proteomics* 11, 1064-1074 (2011).
72. Geer, L. Y. et al. Open mass spectrometry search algorithm. *J. Proteome Res.* 3, 958-964 (2004).
73. Taus, T. et al. Universal and confident phosphorylation site localization using phosphoRS. *J. Proteome Res.* 10, 5354-5362 (2011).

74. Sadowski, I. et al. The PhosphoGRID *Saccharomyces cerevisiae* protein phosphorylation site database: version 2.0 update. *Database* 2013, bat026-bat026 (2013).
75. Chou, M. F. & Schwartz, D. Biological sequence motif discovery using motif-x. *Curr Protoc Bioinformatics* 5 Chapter 13, Unit 13.15-24 (2011).
76. Schwartz, D. & Gygi, S. P. An iterative statistical approach to the identification of protein phosphorylation motifs from large-scale data sets. *Nat Biotechnol* 23, 1391-1398 (2005).
77. Chatr-aryamontri, A. et al. The BioGRID interaction database: 2017 update. 45, D369-D379 (2017).
78. Sharifpoor, S. et al. A quantitative literature-curated gold standard for kinase-substrate pairs. *Genome Biol* 12, R39 (2011).
79. MacGilvray, M. E. et al. Network inference reveals novel connections in pathways regulating growth and defense in the yeast salt response. *bioRxiv* 176230 (2017). doi:10.1101/176230
80. Thij s, G. et al. A Gibbs sampling method to detect overrepresented motifs in the upstream regions of coexpressed genes. *J Comput Biol* 9, 447-464 (2002).
81. Schwalbach, M. S. et al. Complex Physiology and Compound Stress Responses during Fermentation of Alkali-Pretreated Corn Stover Hydrolysate by an *Escherichia coli* Ethanologen. *Appl Environ Microbiol* 78, 3442-3457 (2012).
82. Heidrich, K. et al. Autophosphorylation-inactivation site of hexokinase 2 in *Saccharomyces cerevisiae*. *Biochemistry* 36, 1960-1964 (1997).
83. Vega, M., Riera, A., Fernandez-Cid, A., Herrero, P. & Moreno, F. Hexokinase 2 Is an Intracellular Glucose Sensor of Yeast Cells That Maintains the Structure and Activity of Mig1 Protein Repressor Complex. *J Biol Chem* 291, 7267-7285 (2016).
84. Ahuatz, D., Riera, A., Peláez, R., Herrero, P. & Moreno, F. HXK2 regulates the phosphorylation state of Mig1 and therefore its nucleocytoplasmic distribution. *J Biol Chem* 282, 4485-4493 (2007).
85. Ludin, K., Jiang, R. & Carlson, M. Glucose-regulated interaction of a regulatory subunit of protein phosphatase 1 with the Snf1 protein kinase in *Saccharomyces cerevisiae*. *Proc Natl Acad Sci USA* 95, 6245-6250 (1998).
86. Thevelein, J. M. & De Winde, J. H. Novel sensing mechanisms and targets for the cAMP—protein kinase A pathway in the yeast *Saccharomyces cerevisiae*. *Molecular Microbiology* 33, 904-918 (1999).
87. Gross, E., Goldberg, D. & Levitzki, A. Phosphorylation of the *S. cerevisiae* Cdc25 in response to glucose results in its dissociation from Ras. *Nature* 360, 762-765 (1992).
88. Jian, D., Aili, Z., Xiaojia, B., Huansheng, Z. & Yun, H. Feedback regulation of Ras2 guanine nucleotide exchange factor (Ras2-GEF) activity of Cdc25p by Cdc25p phosphorylation in the yeast *Saccharomyces cerevisiae*. *FEBS Lett* 584, 4745-4750 (2010).
89. Gross, A., Winograd, S., Marbach, I. & Levitzki, A. The N-terminal half of Cdc25 is essential for processing glucose signaling in *Saccharomyces cerevisiae*. *Biochemistry* 38, 13252-13262 (1999).
90. Jackson, S. P., Downs, J. A. & Lowndes, N. F. A role for *Saccharomyces cerevisiae* histone H2A in DNA repair. *Nature* 408, 1001-1004 (2000).
91. Li, X. et al. Comparison of xylose fermentation by two high-performance engineered strains of *Saccharomyces cerevisiae*. *Biotechnol Rep (Amst)* 9, 53-56 (2016).
92. Lee, S.-M., Jellison, T. & Alper, H. S. Systematic and evolutionary engineering of a xylose isomerase-based

- pathway in *Saccharomyces cerevisiae* for efficient conversion yields. *Biotechnol Biofuels* 7, 122 (2014).
93. Kim, S. R. et al. Rational and Evolutionary Engineering Approaches Uncover a Small Set of Genetic Changes Efficient for Rapid Xylose Fermentation in *Saccharomyces cerevisiae*. *PLoS ONE* 8, e57048 (2013).
94. Zhou, H., Cheng, J.-S., Wang, B. L., Fink, G. R. & Stephanopoulos, G. Xylose isomerase overexpression along with engineering of the pentose phosphate pathway and evolutionary engineering enable rapid xylose utilization and ethanol production by *Saccharomyces cerevisiae*. *Metab Eng* 14, 611-622 (2012).
95. Cadete, R. M. et al. Exploring xylose metabolism in *Spathaspora* species: XYL1.2 from *Spathaspora passalidarum* as the key for efficient anaerobic xylose fermentation in metabolic engineered *Saccharomyces cerevisiae*. *Biotechnol Biofuels* 9,167 (2016).
96. Runquist, D., Hahn-Hagerdal, B. & Bettiga, M. Increased ethanol productivity in xylose-utilizing *Saccharomyces cerevisiae* via a randomly mutagenized xylose reductase. *Appl Environ Microbiol* 76, 7796-7802 (2010).
97. Drgon, T., Sabová, L., Nelson, N. & Kolarov, J. ADP/ATP translocator is essential only for anaerobic growth of yeast *Saccharomyces cerevisiae*. *FEBS Lett* 289, 159-162 (1991).
98. Abramova, N., Sertil, O., Mehta, S. & Lowry, C. V. Reciprocal regulation of anaerobic and aerobic cell wall mannoprotein gene expression in *Saccharomyces cerevisiae*. *J Bacteriol* 183, 2881-2887 (2001).
99. Camarasa, C., Faucet, V. & Dequin, S. Role in anaerobiosis of the isoenzymes for *Saccharomyces cerevisiae* fumarate reductase encoded by OSM1 and FRDS1. *Yeast* 24, 391-401 (2007).
100. Rachidi, N., Martinez, M. J., Barre, P. & Blondin, B. *Saccharomyces cerevisiae* PAU genes are induced by anaerobiosis. *Molecular Microbiology* 35, 1421-1430 (2002).
101. Linde, ter, J. J. et al. Genome-wide transcriptional analysis of aerobic and anaerobic chemostat cultures of *Saccharomyces cerevisiae*. *JBacteriol* 181, 7409-7413 (1999).
102. Wilcox, L. J. Transcriptional Profiling Identifies Two Members of the ATP-binding Cassette Transporter Superfamily Required for Sterol Uptake in Yeast. *J Biol Chem* 277, 32466-32472 (2002).
103. Sertil, O., Cohen, B. D., Davies, K. J. & Lowry, C. V. The DAN1 gene of *S. cerevisiae* is regulated in parallel with the hypoxic genes, but by a different mechanism. *Gene* 192, 199-205 (1997).
104. Skoneczny, M. & Rytka, J. Oxygen and haem regulate the synthesis of peroxisomal proteins: catalase A, acyl-CoA oxidase and Pexlp in the yeast *Saccharomyces cerevisiae*; the regulation of these proteins by oxygen is not mediated by haem. *Biochemical Journal* 350, 313-319 (2000).
105. Luo, Z. & van Vuuren, H. J. J. Functional analyses of PAU genes in *Saccharomyces cerevisiae*. *Microbiology* 155, 4036-4049 (2009).
- What is claimed is:
1. A recombinant yeast genetically engineered to ferment xylose and exhibit a decreased level of BCY1 (a regulatory subunit of protein kinase A) protein activity, wherein the recombinant yeast provides increased rate of anaerobic xylose fermentation in the yeast relative to a recombinant yeast having the same genetic background but not exhibiting a decreased level of BCY1 protein activity wherein the recombinant yeast is *Saccharomyces cerevisiae* comprising

45

a degradable tag operably linked to BCY1 to decrease levels of BCY1 protein activity and engineered to lack BCY1 protein activity by a mutation in the recombinant yeast's BCY1 gene.

2. The recombinant yeast of claim 1, wherein the recombinant yeast exhibits reduced cell growth as compared to a recombinant yeast having the same genetic background but not exhibiting a decreased level of BCY1 protein activity.

3. The recombinant yeast of claim 1, wherein the recombinant yeast produces ethanol at an increased rate relative to a recombinant yeast not exhibiting decreased levels of BCY1 protein activity.

4. The recombinant yeast of claim 3, wherein the increased rate of ethanol production occurs under anaerobic conditions.

5. A yeast inoculum, comprising: (a) a recombinant yeast of claim 1; and (b) a culture medium.

6. A method for producing ethanol by anaerobic fermentation of xylose in yeast, comprising: (a) culturing under ethanol-producing conditions a recombinant yeast genetically engineered to ferment xylose and to exhibit a decreased level of BCY1 (a regulatory subunit of protein

46

kinase A) protein activity, wherein the recombinant yeast provides increased rate of anaerobic xylose fermentation in the yeast relative to a recombinant yeast having the same genetic background but not exhibiting a decreased level of BCY1 protein activity; and (b) isolating ethanol produced by said recombinant yeast wherein the recombinant yeast is *Saccharomyces cerevisiae* comprising a degradable tag operably linked to BCY1 to decrease levels of BCY1 protein activity and engineered to lack BCY1 protein activity by a mutation in the recombinant yeast's BCY1 gene.

7. The method of claim 6, wherein the recombinant yeast exhibits reduced cell growth as compared to a recombinant yeast having the same genetic background but not exhibiting a decreased level of BCY1 protein activity.

8. The method of claim 6, wherein the recombinant yeast produces ethanol at an increased rate relative to a recombinant yeast not exhibiting decreased levels of BCY1 protein activity.

9. The method of claim 8, wherein the increased rate of ethanol production occurs under anaerobic conditions.

* * * * *